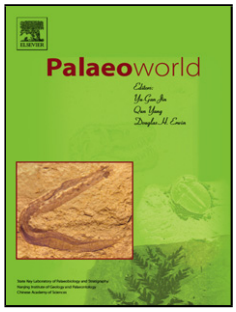


Title: Brachiopods from the Cisuralian–Guadalupian of Darvaz, Tajikistan and implications for Permian stratigraphic correlations

Author: Lucia Angiolini Mark Campagna Letizia Borlenghi Tatiana Grunt Daniel Vachard Giovanni Vezzoli Irene Vuolo James Worthington Alda Nicora Andrea Zanchi

PII: S1871-174X(16)30024-5
DOI: http://dx.doi.org/doi:10.1016/j.palwor.2016.05.006
Reference: PALWOR 371

To appear in: *Palaeoworld*

Received date: 1-12-2015
Revised date: 24-4-2016
Accepted date: 16-5-2016

Please cite this article as: Angiolini, L., Campagna, M., Borlenghi, L., Grunt, T., Vachard, D., Vezzoli, G., Vuolo, I., Worthington, J., Nicora, A., Zanchi, A.,Brachiopods from the CisuralianndashGuadalupian of Darvaz, Tajikistan and implications for Permian stratigraphic correlations, *Palaeoworld* (2016), http://dx.doi.org/10.1016/j.palwor.2016.05.006

# Brachiopods from the Cisuralian–Guadalupian of Darvaz, Tajikistan and implications for Permian stratigraphic correlations

Lucia Angiolini [a] *, Mark Campagna [a], Letizia Borlenghi [a], Tatiana Grunt [b], Daniel Vachard [c], Giovanni Vezzoli [d], Irene Vuolo [a], James Worthington [e], Alda Nicora [a], Andrea Zanchi [d]

[a] Dipartimento di Scienze della Terra "A. Desio", Via Mangiagalli 34, 20133 Milano, Italy

[b] Laboratory-Studio "Living Earth", Moscow, Russia

[c] 1 rue des Tilleuls, 59152 Gruson, France

[d] Dipartimento di Scienze dell'Ambiente e del Territorio e di Scienze della Terra, Piazza della Scienza 4, 20126 Milano, Italy

[e] Department of Geosciences, The University of Arizona, 1040 E. 4th Street, Tucson, AZ 85721, USA

* Corresponding author. *E-mail address*: lucia.angiolini@unimi.it

**Abstract**

In this paper, we describe the upper Cisuralian Safetdara and Gundara formations of the Darvaz mountains, North Pamir, which were part of the Kunlun Arc, developed along the active Eurasian margin. The Safetdara Formation comprises massive limestones (mainly cyanobacterial, *Tubiphytes* and *Archaeolithoporella* boundstones) alternating with well-bedded bioclastic and oncoidal limestones) and an interval of recessive shales. The formation crops out above the Chelamchi Formation consisting of turbiditic siltstones and sandstones with bioclastic silty limestones yielding massive limestone olistoliths. The Gundara Formation consists of fine sandstones at the base, followed by well-bedded marly bioclastic, oncoidal and microbial limestones, bearing a rich silicified brachiopod fauna in life-position. Two new taxa have been identified in this association: the cemented coralliform *Gundaria insolita* n. gen. n. sp. and the pedicle attached *Hemileurus politus* n. sp. The inferred environmental setting is that of shoal deposits of warm, shallow, high energy, clear marine waters for the Safetdara Formation. The agglutinated microbial reefs to cluster reefs of the Gundara Formation were probably growing in a muddier, quieter and probably slightly deeper setting.

The foraminifers of the *Brevaxina* Zone suggest a Bolorian age for the top of the Chelamchi Formation, the Safetdara Formation and the base of the Gundara Formation. Kungurian conodonts have been found in the lower part of the Safetdara Formation. The biostratigraphic data from the sedimentary succession of North Pamir, integrated with those already obtained from Southeast Pamir, allow to refine the correlations between the Tethyan regional scale and the International Time Scale. In particular, it seems now clear that the Bolorian and the lower part of the Kubergandian correlate to the Kungurian.

**Keywords:** Tethyan scale; Bolorian; Kungurian; biostratigraphy; palaeoecology

## 1. Introduction

The remote Pamir mountains in Tajikistan are characterized by spectacular upper Palaeozoic–Mesozoic sedimentary successions, which record the evolution of the Cimmerian blocks from their rift from Gondwana to their collision to Eurasia (Angiolini et al., 2013, 2015 and references therein), and represent the stratotypes of certain regional stages of the Tethyan Scale. Although accessing these successions is challenging due to logistical difficulties, studying them is very important both for constraining the motions of the Cimmerian terranes and their collision to Eurasia (and consequently the evolution of the Palaeotethys/Neotethys Ocean) and for understanding the correlation of the regional Tethyan Scale to the International Stratigraphic Scale, specifically for the Permian.

As shown by Angiolini et al. (2015, fig. 18), there is a striking difference among the blocks that comprise the Pamirs. Whereas the North Pamir represents the former Eurasian margin, the Central Pamir and South Pamir were part of the Cimmerian belt during the Permian and the Triassic and therefore separated from North Pamir by the Palaeotethys Ocean. Beginning in the late Triassic, a cascade of complex geodynamic events transpired: the accretion of the Central Pamir to the North Pamir, the accretion of the South Pamir to the Central Pamir along the Rushan-Pshart suture, and slightly later, the collision of Karakoram to South Pamir along the Tirich Boundary Zone. Although the tectonic and sedimentary evolution of South Pamir (and particularly the Southeast Pamir) has been previously documented (e.g., Dronov and Leven, 1990; Vlasov et al., 1991; Schwab et al., 2004; Robinson et al., 2012; Angiolini et al., 2013, 2015), the North Pamir, which underwent a very complex tectonic evolution from the

Carboniferous onward (Leven and Shcherbovich, 1978; Leven, 1981, 1997; Leven et al., 1983, 1992), is comparatively poorly documented.

Here, we focus on part of the Permian succession in the North Pamir with the aim of: 1) establishing a detailed biostratigraphy and chronostratigraphy based on foraminifers and conodonts; 2) constraining the correlation of the Tethyan scale (Leven, 1980) to the International Stratigraphic Scale, in particular extending the correlation already performed in SE Pamir (Angiolini et al., 2015) to the late Early Permian (Bolorian); and 3) describing the spectacularly preserved silicified brachiopod fauna of the Gundara Formation, which contains new taxa.

## 2. Geological setting

The fossil associations investigated herein were collected in the Gundara valley, which is situated south of the village of Mionadus in the Obikhingou valley in the Darvaz mountains of the North Pamir (Figs. 1, 2).

The Darvaz belt forms the NE margin of the North Pamir's Kunlun Arc, which is part of the Eurasian domain, extending from NW to SE between the Darvaz Fault and the intra-Pamir Kunlun suture (Fig. 1). The active, left-lateral Darvaz Fault (Burtman and Molnar, 1993) represents the western boundary of the Pamir indenter (Reiter et al., 2011). This fault juxtaposes the Palaeozoic–Triassic units of the North Pamir with the Mesozoic–Cenozoic successions of the Tajik basin, now exposed in the Peter the First range (Hamburger et al., 1992) south of the Garm block of the South Tien Shan. The intra-Pamir Kunlun suture (Schwab et al., 2004) divides the northernmost portion of the Pamir (Kunlun) from the Karakul-Mazar arc complex, which was active primarily from the Permian–Triassic along the southern margin of the North Pamir. The Karakul-Mazar arc is, in turn, thrust southward onto the Gondwana-derived Central Pamir bock along the Tanymas thrust, which reactivated the Mesozoic North-Central Pamir suture zone. This suture, separating the Mazar-Karakul arc terranes from Central Pamir, has been often correlated with the Jinsha suture of Tibet (Schwab et al., 2004; Angiolini et al., 2013; Robinson, 2015). However, recent studies in Tibet (Zhang et al., 2015; Zhai et al., 2016) suggest that the main suture marking the subduction of the Palaeotethys Ocean was the Longmu-Co Shuanghu, separating North from South Pamir, whereas the Jinsha Suture is now interpreted as a secondary branch of the Palaeotethys Ocean. For this reason, we prefer to avoid a direct correlation between the North-Central Pamir suture zone and the Jinsha Suture.

The study area is situated in the southwestern Darvaz range and primarily comprises arc-related Carboniferous–Triassic volcano-sedimentary successions. Abundant Carboniferous lava flows occur at the base of the succession along the Charymdara valley (Leven, 2012) and pass up-section into coarse clastic deposits and mixed terrigenous carbonate units, which we investigate herein (Figs. 2, 3). This entire succession is thrust over the Jurassic, Cretaceous and Cenozoic successions of the Tajik basin. According to previous studies (Ruzhentsev et al., 1977; Ruzhentsev and Shol'man, 1982; Schwab et al., 2004; Leven, 2012), the upper Palaeozoic succession rests on mélange-type, serpentinite-bearing units exposed in the Kalaikumb area, which are interpreted as the remnants of a back-arc basin developed along the southern Eurasian margin.

The Permian succession investigated herein generally dips NW and strikes parallel to the Darvaz range's regional NE–SW structural fabric, showing a marked oroclinal bending of the belt's structural fabric in front of the India–Pamir indenter. Different research groups have interpreted the succession exposed in the upper part of the Gundara valley in different ways. Leven (1981) claims that the Permian–Triassic succession is stratigraphically continuous, but the Soviet 1:200,000 geologic maps of Tajikistan show a tectonic repetition of the Permian units north of the outcrops of the Gundara Formation (Fig. 2). Leven (2012) also suggests the occurrence of Carboniferous sediments in the upper Zydadara valley, however, which contradicts his previous interpretations (Leven, 1967, 1981). In Fig. 2, we suggest the possible occurrence of a fault bounding the Gundara Formation to the north, as indicated by the presence of vertical thin-bedded turbiditic sandstones that pass stratigraphically upward to massive limestones. Soviet 1:200,000 geologic maps indicate that most of the Permian to Triassic succession is unconformably sealed by the Jurassic succession (with coal locally occurring at its base), which suggests that the primary deformation event occurred in the area before the Jurassic. Andesitic dikes and stocks, attributed in the literature to the Early Jurassic, are widespread in the area. Another major unconformity is well-defined at the top of the Gundara valley between the Permian successions and the Neogene units, which form the southernmost portion of the Tajik basin (Fig. 2).

We measured and sampled two stratigraphic sections in pursuit of our research goals:

1) The Bolorian stratotype at the junction of the watersheds between the Charymdara, Zydadara and Gundara valleys (38°45’34’’N, 70°53’27’’E; 3420 m a.s.l. at the base of the section) (Table 1, Figs. 2-4, 6). Leven (1979) proposed that the top of the Tchelamchi Formation, the Safetdara Formation and the base of the Gundara Formation together comprise the stratotype of the Bolorian stage of the Tethyan Scale. It was described in subsequent publications by Leven et al. (1983, 1992) and Filimonova (2008);
2) A short log in the Kubergandian Gundara Formation along the left side of the Gundara valley (38°45’45.1’’N, 70°52’49.9’’E; 3542 m a.s.l.) (Figs. 2, 3, 5, 6). Its rich fossil brachiopod fauna was studied by Grunt (1986), Smirnova and Grunt (2003) and Smirnova (2007).

**3. Stratigraphic framework**

We measured Permian stratigraphic sections in the eastern Darvaz region, which, according to Leven and Shcherbovich (1978, 1980), Leven et al. (1983, 1992), and Leven (1997), comprises (Fig. 3):

- the Asselian–lower Sakmarian Sebisurkh Formation, which comprises bioclastic limestones (up to 450 m);
- the Sakmarian-Yakhtashian Khoridzh Formation, which comprises turbiditic shales and sandstones (300–750 m);
- the Yakhtashian Zygar Formation, which comprises volcaniclastic conglomerates, sandstones and shales (300–400 m);
- the Yakhtashian–lower Bolorian Chelamchi Formation, which comprises alternating claystones, siltstones, sandstones, conglomerates, and reefal limestones (up to 1000 m; 390 m at the stratotype);
- the uppermost Yakhtashian–Bolorian Safetdara Formation, which comprises reefal limestones (up to 900 m; 360 m at the stratotype);
- the upper Bolorian–Kubergandian Gundara Formation, which comprises sandstones, shales and limestones (up to 870 m);
- the Murgabian Daraitang Formation, which comprises multicoloured tuffs (800 m);

- the Murgabian Valvaljak Formation, which comprises volcaniclastic red sandstones and conglomerates (> 1000 m);
- the Midian Kaftarlmol Formation, which comprises gypsum (at the base), sandstones, and shales (400 m);
- the Midian–Dzhulfian Kafirbacha Formation, which comprises carbonates and shales (50–230 m).

The succession in the western Darvaz region is similar, with the notable difference that the Gundara Formation is replaced by the multi-colored volcaniclastic and terrigenous deposits of the Kuljaho Formation.

As indicated above, we studied the Safetdara and Gundara formations at the watersheds between the Charymdara, Zydadara and Gundara valleys (Bolorian stratotype) and along the left bank of the Gundara valley (Fig. 2). A detailed description of the lithology and microfacies of the Bolorian stratotype section is given in Table 1. We also investigated five samples from the upper part of the Chelamchi Formation at the base of the Bolorian stratotype.

The upper 130 m of the Chelamchi Formation (Figs. 2, 6) consist of poorly outcropping turbiditic siltstones and sandstones with bioclastic silty limestones (bioclastic and intraclastic floatstones), yielding olistoliths of massive limestone olistoliths (*Tubiphytes* and *Archaeolithoporella* boundstones, locally with well-developed botryoid cement). Sandstones are characterized by abundant twinned and sericitized plagioclase, monocrystalline quartz, biotite and minor chloritized mafic volcanic rock fragments (Fig. 7).

The Safetdara Formation primarily comprises massive limestones that alternate with well-bedded bioclastic limestones and an interval of recessive shales (Table 1, Figs. 4, 6). The microfacies consist of bioclastic and oncoidal grainstones, floatstones, and rudstones and of boundstones produced by cyanobacterial microbialites, *Tubiphytes* and *Archaeolithoporella*. Boundstones with rugose corals occur at the top of the formation.

The Gundara Formation is characterized by fine sandstones at its base, overlain by 10–40 cm-thick marly bioclastic limestone beds that locally bear a rich silicified biota (Figs. 5, 6). The sandstones contain twinned and sericitized plagioclase, monocrystalline quartz, chloritized mafic-volcanic lithic fragments, carbonate grains

and rare biotite. (Fig. 7). The presence of bioclastic wackestones in the Gundara Formation distinguishes it from the Safetdara Formation. These formations are similar with respect to their microfacies and the presence of oncoidal and bioclastic floatstones, bioclastic grainstones and microbial boundstones.

## 4. Palaeoecology

Our microfacies analysis of samples from the Safetdara Formation reveals that they contain mainly photozoan assemblages. Therefore, they are typical shoal deposits of warm, shallow (5–10 m deep) and agitated but clear marine waters. The local occurrence of a beach rock particularly enriched in well-preserved calcareous algae for the Safetdara Formation (e.g., TJ171) testifies to a very shallow marine depositional environment. The inferred environment for the Gundara Formation is similar but muddier, quieter and likely slightly deeper.

### *4.1. Brachiopod palaeocology*

The occurrence of brachiopods, which are particularly abundant in the Gundara Formation, enables us to reliably constrain palaeoecological and palaeoenvironmental variables and derive enhanced interpretations from them.

The brachiopods of the Safetdara Formation are scattered among the photozoan assemblages and comprise both free-living and ubiquitous pedicle-attached species. The *Larispirifer* sp. indet. specimens in TJ181 are remarkable for their large size and are disarticulated, which suggests winnowing or transport. They were probably able to attain such a large size and thick shell due to an abundant food supply, which is favorable for the growth of spiral lophophore bearers (Perez-Huerta and Sheldon, 2006).

The rich silicified brachiopod fauna from the Gundara Formation is noteworthy. The Gundara Formation comprises 534 specimens of exclusively attached forms, both shelly-attached reef dwellers (22%) and pedicle-attached taxa (78%), forming life (TJ192, TJ193, TJ194, TJ197, TJ198) to neighborhood (TJ195, TJ199) assemblages. The specimens of the shelly attached *Gundaria insolita* n. gen. n. sp. were fixed to a hard substrate, possibly provided by microbial boundstones coupled with cementation of the umbo and by rhizhoid spines, which would have provided stability. Ubiquitous pedicle attached species comprise *Hemileurus politus* n. sp., *Posicomta gundarensis*, *Orbicoelia* sp. indet., *Spiriferellina* sp. indet., *Paraspiriferina* sp. indet.,

*Fredericksolasma lata*, *Fredericksolasma rhomboidalis*, and *Fredericksolasma* sp. indet.

Our preferred palaeoenvironmental reconstruction is one of agglutinated microbial reefs to cluster reefs (e.g., Riding, 2002). The microbial reefs are formed by the cyanobacterial microbialites *Tubiphytes* and *Archaeolithoporella*, with a few large cavities filled by botryoidal cements and subordinate skeletal elements. The cluster reefs are made by in-place conical skeletons of *Gundaria insolita* n. gen. n. sp. that were adjacent but not always in contact with the substrate. The *Gundaira insolita* were also able to trap loose sediment, which indicates that the reefs are matrix-supported. In-place, pedicle-attached species contributed to the framework and helped trap the matrix. These reefs were likely laterally extensive despite their low topographic relief, which is consistent with the mostly bedded nature of the Gundara Formation. The abundance of matrix and the reduced cementation and bioerosion suggest muddy depositional environments, which were probably deeper and more turbid than those of the Safetdara Formation.

## 5. Bio-chronostratigraphy of the Safetdara and Gundara formations

### *5.1. Conodonts*

Thirty samples for conodonts were collected from the Safetdara and Gundara formations in the study area. However, after processing, only a few conodonts were recovered from sample TJ163, in the lower part of the Safetdara Formation.

One of the recovered specimens belongs to *Sweetognathus modulatus* Chernykh, 2006 (Fig. 8), being characterized by high carinae parallel to the lateral margin, consisting of 6-7 denticles of the same height and symmetrically disposed; the ornamentation is pustulose; the blade is missing and only some nodes are preserved on the anteriormost end of the platform; the basal cavity is symmetric, even if part of the inner margin is lacking. This species differs from *Sweetognathus whitei* (Rhodes) by the carinae teeth. In *S. whitei* the teeth are bell-shaped with a remarkable medium pitch, whereas in *S. modulatus* the teeth are nearly subquadrate. Yet, the median ridge on *S. whitei* is much better developed. *S. modulatus* differs from *Sweetognathus rhomboides* Chernykh by its narrower carinae which are parallel to the lateral edges.

The holotype of *S. modulatus* comes from Bed 3, Saranin Horizon, Aleksandrov Formation, Zhil-Tau Section, Zhaksy-Kargala River, Aktyubinsk region of Kazakhstan and it is Kungurian in age (Chernykh, 2006).

The other two specimens were identified as *Sweetognathus* sp. because they lack the main diagnostic features of the species, such as those of the carinae and the pustulose ornamentations.

None of the samples collected from the Gundara Formation yielded conodonts.

*5.2. Foraminifers*

The Safetdara Formation is particularly rich in smaller foraminifers and primitive neoschwagerinoid (Figs. 9, 15; Appendices 1, 2).

Staffelloid and Schubertelloid fusulinids are represented by *Neofusulinella pseudogiraudi* (Sheng, 1962 non 1963) and are quite rare in the Safetdara Formation. The schwagerinoid fusulinids are represented by species of *Darvasites*, *Leeina*, *Darvasella* and *Shichatenella*. Among the primitive Neoschwagerinoidea, four taxa of misellinins occur successively along the section: small *Brevaxina dyhrenfurthi otai* (Sakaguchi and Sugano, 1966) – *B. dyhrenfurthi* (Dutkevich in Likharev et al., 1939) – *B. parvicostata* (Deprat, 1915) – *Brevaxina* sp. 1 transitional to the first true *Misellina*, i.e., *M. termieri* (Deprat, 1915). The misellinins are very rare from bed TJ184 upward, occurring only sporadically. In this study, we use the genus name *Brevaxina* for spherical species of misellinins, whereas we restrict the name *Misellina* to more ovate misellinins. The characteristic shape of *Misellina* is based on the shape of the type species *Misellina ovalis* (Deprat, 1915), because *ovalis* means ovate in Latin. In fact, *Brevaxina* is transitional between the nautiloid ancestor *Pamirina* and the ovate to inflated fusiform descendent *Misellina* (sensu stricto). Some species are, in turn, transitional between *Brevaxina* and *Misellina*. This is the case for *Brevaxina parvicostata*, whose diameter/width ratio is 1.1 (only slightly greater than the theoretical ratio of 1 for the spherical *Brevaxina*). It is noteworthy that although the species *parvicostata* has been generally assigned to *Misellina* by most authors, it has been already placed in *Brevaxina* by Rozovskaya (1975) and by Lys (1994), who revised the type material of Deprat (1915).

Interestingly, the genus *Levenella* (= *Levenia* Ueno, 1991a, pre-occupied), which is the ancestor of *Pamirina* and therefore also of *Brevaxina*, is abundant in most of the section (from TJ171 to TJ184), where it is represented by at least two species: *Levenella* aff. *leveni* (Kobayashi, 1977) and *Levenella* sp. 2. This genus is generally absent from the Bolorian of Japan (Ueno, 1991b) and, where present, only occurs at the base of this stage (Ueno, 1996b).

The foraminifer assemblages of the topmost 100 m of the Chelamchi Formation and the first few meters of the Gundara Formation are essentially identical to the fauna of the Safetdara Formation. This similarity was highlighted by Leven et al. (1983), who found *Brevaxina dyhrenfurthi* in the upper 130 m of the Chelamchi Formation.

Based on the occurrence of *Neofusulinella pseudogiraudi* (Sheng, 1962 not 1963), and the four species of *Brevaxina*, the stratotype section of the Bolorian (comprising the upper 130 m of the Chelamchi Formation, all the Safetdara Formation and the very base of the Gundara Formation) corresponds to a single biozone, the *Brevaxin*a Zone (Fig. 16). This is confirmed by the absence of *Neofusulinella giraudi* Deprat, 1915 (the descendent of *N. pseudogiraudi*) which characteristically appears in the *Misellina* Zone (Vachard et al., 2013).

The base of the stratigraphically higher *Misellina* Zone (Kubergandian) may be identified in bed TJ187, which is characterized by the FO of *Shichatenella gundarensis* (Kalmykova, 1960). Moreover, this bed is located above the occurrence of transitional forms of *Brevaxina* sp. 1 to *Misellina termieri* (TJ182–183). So the Bolorian-Kubergandian boundary may be identified in the lower part of the Gundara Formation.

### *5.3. Brachiopods*

Brachiopods cannot contribute significantly to the age assignment because they are represented by species of genera that widely span the Early to Middle Permian. The brachiopods collected in the Gundara Formation comprise, among others, a new species of the genus *Hemileurus* which is known only from the Lower Permian Neal Ranch Formation of Texas (Cooper and Grant, 1976), and from the Kungurian Tunglonggongba Formation of Domar, Tibet (Jin and Sun, 1981). Three other species, *Posicomta gundarensis*, *Fredericksolasma rhomboidalis* and *Fredericksolasma lata*, have been only recorded in the Gundara Formation (Grunt, 1986; Smirnova and Grunt, 2003; Smirnova, 2007).

## 6. Implications for Permian correlation

Our redescription of the Bolorian stratotype has important implications for correlating the Tethyan regional chronostratigraphic scale (Leven, 1980) with the International (Global) scale.

As recently summarized in Davydov et al. (2013) and Angiolini et al. (2015), the two lower stages of the Tethyan scale, the Asselian and the Sakmarian, which come from the Urals scale (Ruzhentsev, 1954; Leven and Shcherbovich, 1978, 1980; Leven et al., 1992; Leven, 2001), should be correlatable to the International Time Scale — though Davydov et al. (2013) contested this. Stratotypes for the two following stages, the Yakhtashian and the Bolorian (Leven, 1979, 1980, 1981; Leven et al., 1983), were selected in the sedimentary successions of the Darvaz region of the North Pamir. The Yakhtashian and its correlation to the Artinskian of the International Time Scale was thoroughly discussed by Leven (2001); however, Davydov et al. (2013) questioned the correlation of the Yakhtashian with the Artinskian. The Bolorian is the object of the present discussion. The following stages are the Kubergandian (Leven, 1963, 1981) and the Murgabian (Miklukho-Maklay, 1958; Leven, 1967, 1981) with stratotypes in the southeast Pamir that were discussed in detail by Angiolini et al. (2015). The final three stages, Midian, Dzhulfian and Dorashamian (Leven, 1980), have stratotypes in Azerbaijan.

Our investigation of the foraminifers from the stratotype section of the Bolorian shows that it comprises a single biozone, the *Brevaxina* Zone, in agreement with previous findings by Ueno (1991b, 1996), Kobayashi (2005) and Davydov et al. (2013), but not with Leven (2001) who included the *Misellina termieri* zone at the top of the Bolorian (Fig. 16). The subsequent *Misellina* Zone with *M. aliciae*, *M. claudiae* and *M. termieri* (≈ *Misellina ovalis-Armenina* Zone) corresponds to the lower Kubergandian (Kobayashi, 2005; Leven, 1998; Davydov et al., 2013; Angiolini et al., 2015).

Correlation with the International Time Scale remains the primary issue, however. In fact, according to Davydov et al. (2013) the Yakhtashian correlates with the upper Artinskian–lower Kungurian, the Bolorian with the upper Kungurian, and the Kubergandian with the Roadian. This contrasts with the findings of Leven and Bogoslovskaya (2006) and Angiolini et al. (2015) who suggested a correlation between the lower Kubergandian and the upper Kungurian and between the Bolorian and the lower–middle Kungurian. Even more problematic is the comparison with the data reported by Shen et al. (2013) from central Japan, who found Kungurian conodonts with lower Murgabian fusulinids (see discussion in Angiolini et al., 2015).

Unfortunately, despite our thorough sampling in the North Pamir, only one conodont sample (TJ163) was productive. This sample was collected at 15 m from the

base of the Safetdara Formation and contains the species *Sweethognathus modulatus*, previously recorded in the Kungurian of Kazakhstan which indicates a Kungurian age for the lower part of the Safetdara Formation.

Combining the present dataset from North Pamir with those collected during investigations in southeast Pamir (Angiolini et al., 2015), we confidently interpret the Bolorian to be equivalent to the Kungurian except for its upper part, which correlates with the Kubergandian (Fig. 16). We note that the discrepancy between our findings and Davydov et al.'s (2013) conclusions, as well as Shen et al.'s (2013) data from central Japan, warrants caution in the implementation of misellinins and cancellinins in biostratigraphic correlations because they indicate endemism and diachroneity.

## 7. Systematic palaeontology: Brachiopoda (by L. Angiolini, M. Campagna, and T. Grunt)

All the described specimens are housed in the Palaeontological Museum of the Department of Earth Sciences "A. Desio", University of Milan, Italy. Specimens are registered with reference number consisting of a prefix MPUM followed by a five digit number. In the paragraphs "material" the field numbers have been added in brackets to each reference number in order to facilitate placement of the specimens along the stratigraphic log; when one reference number includes more than one specimen, their number is indicated in round brackets. In the figure captions only the reference number is indicated.

The systematic study follows the classifications of Brunton et al. in Williams et al. (2000) for the productids, Savage et al. in Williams et al. (2002) for the rhynchonellids, Alvarez and Rong in Williams et al. (2002), Alvarez in Williams et al. (2007) for the athyridids, Johnson et al. in Williams et al. (2006) for the ambocoelioids, Carter in Williams et al. (2006) for the spiriferoids and pennospiriferoids and Jin et al. in Williams et al. (2006) for the dielasmatoids.

All the tables of dimensions are in Appendix 3.

Order PRODUCTIDA Sarytcheva and Sokolskaya, 1959
Superfamily RICHTHOFENIOIDEA Waagen, 1885
Family CYCLACANTHARIIDAE Cooper and Grant, 1975
Subfamily CYCLACANTHARIINAE Cooper and Grant, 1975

Genus *Gundaria* n. gen.

**Type species:** *Gundaria insolita* n. sp.

**Etymology:** From the Gundara valley, Darvaz, North Pamir, Tajikistan.

**Diagnosis:** Cyclacanthariinae with a geniculated dorsal valve, a lobed ventral muscle callosity, the lower part of the cone filled by cystose shell and no coscinidium, but a rim of protective spines.

**Remarks:** *Gundaria* n. gen. differs from *Cyclacantharia* Cooper and Grant, 1969 by its lobate ventral callosity, by the apex of the cone strongly thickened by cystose shell and by the absence of long endospines inside the dorsal valve. Also, the rim of protective spines around the inner margin of the cup is less developed, with spines growing upward rather than medianly and the dorsal valve has a short geniculated trail which seems to be absent in *Cyclacantharia*. The new genus differs from the other genera of the subfamily the absence of a coscinidium.

*Hercosia* Cooper and Grant, 1969 of the family Hercosiidae may appear similar in shape and size to *Gundaria* n. gen.; however, *Hercosia* is readily distinguished by its well defined median septum, which is totally absent in *Gundaria* n. gen.

*Gundaria insolita* n. gen. n. sp.

(Figs. 17, 18, 20, 21)

**Types:** Holotype: MPUM 11421 [TJ199-C]. Paratypes: MPUM 11410 [TJ195-A]; MPUM 11411 [TJ195-B]; MPUM 11412 [TJ195-C]; MPUM 11413 [TJ195-D]; MPUM 11414 [TJ195-E]; MPUM 11415 [TJ195-F]; MPUM 11416 [TJ195-G]; MPUM 11417 [TJ195-H]; MPUM 11418 [TJ195-I]; MPUM 11419 [TJ199-A]; MPUM 11420 [TJ199-B]; MPUM 11422 [TJ199-D]; MPUM 11423 [TJ199-E]; MPUM 11424 [TJ199-F]; MPUM 11425 [TJ199-G]; MPUM 11426 [TJ199-H]; MPUM 11427 [TJ199-I]; MPUM 11428 [TJ199-L]; MPUM 11429 [TJ199-M]; MPUM 11430 [TJ199-N]; MPUM 11431 [TJ199-O].

**Etymology:** From the Latin insolitus-a-um, unusual.

**Material:**

16 Articulated specimens: MPUM 11432 [TJ192]; MPUM 11433 [TJ194]; MPUM 11434 [TJ195]; MPUM 11417 [TJ195-H]; MPUM 11418 [TJ195-I]; MPUM 11420 [TJ199-B]; MPUM 11421 [TJ199-C]; MPUM 11423 [TJ199-E]; MPUM 11426 [TJ199-H]; MPUM 11427 [TJ199-I]; MPUM 11435 [TJ199 (4 specimens)]; MPUM

11524 [TJ195]; MPUM 11525 [TJ199].

104 Ventral valves: MPUM 11432 [TJ192 (2 specimens)]; MPUM 11433 [TJ194 (2 specimens)]; MPUM 11410 [TJ195-A]; MPUM 11411 [TJ195-B]; MPUM 11412 [TJ195-C]; MPUM 11413 [TJ195-D]; MPUM 11414 [TJ195-E]; MPUM 11415 [TJ195-F]; MPUM 11416 [TJ195-G]; MPUM 11434 [TJ195 (44 specimens)]; MPUM 11419 [TJ199-A]; MPUM 11422 [TJ199-D]; MPUM 11424 [TJ199-F]; MPUM 11425 [TJ199-G]; MPUM 11428 [TJ199-L]; MPUM 11429 [TJ199-M]; MPUM 11430 [TJ199-N]; MPUM 11435 [TJ199 (42 specimens)].

2 Clusters: MPUM 11431 [TJ199-O]; MPUM 11436 [TJ199].

Several fragments: MPUM 11433 [TJ194]; MPUM 11434 [TJ195]; MPUM 11435 [TJ199].

Figured specimens: MPUM 11410 [TJ195-A]; MPUM 11411 [TJ195-B]; MPUM 11412 [TJ195-C]; MPUM 11413 [TJ195-D]; MPUM 11414 [TJ195-E]; MPUM 11415 [TJ195-F]; MPUM 11416 [TJ195-G]; MPUM 11417 [TJ195-H]; MPUM 11418 [TJ195-I]; MPUM 11419 [TJ199-A]; MPUM 11420 [TJ199-B]; MPUM 11421 [TJ199-C]; MPUM 11422 [TJ199-D]; MPUM 11423 [TJ199-E]; MPUM 11424 [TJ199-F]; MPUM 11425 [TJ199-G]; MPUM 11426 [TJ199-H]; MPUM 11427 [TJ199-I]; MPUM 11428 [TJ199-L]; MPUM 11429 [TJ199-M]; MPUM 11430 [TJ199-N]; MPUM 11431 [TJ199-O]; MPUM 11524 [TJ195]; MPUM 11525 [TJ199].

**Stratigraphic occurrence:** TJ192, TJ194, TJ195, TJ199 from the Gundara Formation

**Diagnosis:** Ventral valve conical, with cone straight or curved, depending on clustering. Dorsal valve flat, anteriorly geniculated, recessed. Lower part of the cone filled by cystose shell. Ventral muscle area forming a 3-lobed mound of cystose shell.

**Description:** Small to medium sized shell; ventral valve conical, variably straight or curved; apical angle: 40–70°; cross section subelliptical to moderately subcircular; height of the cone: 18–31 mm, width of the section: 18–26 mm. Dorsal valve flat, anteriorly geniculated, quite deeply recessed into the ventral one, with narrow hinge and short neck. Marginal rim of the ventral valve above the dorsal valve rarely preserved and characterized by spine bases growing up along the internal wall of the valve. Ornamentation of the ventral valve of rhizoid spines that could be long and thick, often directed downwards and growth lines (Appendix 4); dorsal valve ornamented by tiny tubercles.

Interior of ventral valve with the lower part of the cone occupied by overlapping shell blisters up to half the height of the cone (Figs. 17, 18); above this cystose shell is

the body chamber. On the floor of the body cavity, there is a lobed mound, generally composed of three lobes and made up of cystose shell (Fig. 17); this represents the muscle attachment area. The body chamber is divided into two cavities by a longitudinal ridge extending from the base of the lobed structure anteriorly to the wall of the chamber opposite the hinge; the ridge is interiorly composed by the blisters extending from the lower part of the valve. The pseudodeltidium is bounded by flat ridges, and the aulacoterma is usually well developed. Numerous tubular internal spines are present, their internal canal crossing the wall of the valve to the shell exterior; they are generally medianly directed.

Interior of dorsal valve with a bilobed cardinal process which projects ventrally, anteriorly supported by a low and short median ridge; muscle scars obscure.

**Discussion:** The shape of the conical ventral valve is variable due to the growth in clusters under the influence of near-growing specimens. Notwithstanding some variation in the apical angle, the shape of the cone and the density of spines inside the ventral valve, the features of the analyzed specimens from the four stratigraphic levels sampled are rather uniform, suggesting that they all belong to the same species.

Order RHYNCHONELLIDA Kuhn, 1949
Superfamily WELLERELLOIDEA Licharew, 1956
Family ALLORHYNCHIDAE Cooper and Grant, 1976

Genus *Hemileurus* Cooper and Grant, 1976

**Type species:** *Hemileurus runcinatus* Cooper and Grant, 1976.

**Remarks:** *Hemileurus* Cooper and Grant, 1976 differs from *Allorhyncus* Weller, 1910 by the pattern of costation; ribs in *Hemileurus* do not start at the umbo, but at about 1/3 of the shell length. *Aldina* Angiolini, 1995 is similar to *Hemileurus* in outline and costation but it has conjunct deltidial plates, whereas *Deltarina* Cooper and Grant, 1976 and *Fascicosta* Stehli, 1955 have a divided hinge plate too, but they are multicostate.

*Hemileurus politus* n. sp.
(Fig. 22A-Ab)

**Etymology:** *politus* because of its few and delayed ribs which give it a smooth

appearance, particularly evident in dorsal view.

**Types:** Holotype: MPUM 11437 [TJ193-4]. Paratypes: MPUM 11438 [TJ195-6]; MPUM 11439 [TJ195-7]; MPUM 11440 [TJ195-8]; MPUM 11441 [TJ195-9]; MPUM 11442 [TJ195-10]; MPUM 11443 [TJ195-11]; MPUM 11444 [TJ199-2]; MPUM 11445 [TJ199-3].

**Material:**

84 Articulated specimens: MPUM 11437 [TJ193-4]; MPUM 11446 [TJ193 (4 specimens)]; MPUM 11441 [TJ195-9]; MPUM 11442 [TJ195-10]; MPUM 11443 [TJ195-11]; MPUM 11447 [TJ195 (65 specimens)]; MPUM 11444 [TJ199-2]; MPUM 11445 [TJ199-3]; MPUM 11448 [TJ199 (9 specimens)].

1 Ventral valve: MPUM 11440 [TJ195-8].

2 Dorsal valves: MPUM 11438 [TJ195-6]; MPUM 11439 [TJ195-7].

7 Fragments: MPUM 11446 [TJ193]; MPUM 11447 [TJ195 (6 specimens)].

Figured specimens: MPUM 11437 [TJ193-4]; MPUM 11438 [TJ195-6]; MPUM 11439 [TJ195-7]; MPUM 11440 [TJ195-8]; MPUM 11441 [TJ195-9]; MPUM 11442 [TJ195-10]; MPUM 11443 [TJ195-11]; MPUM 11444 [TJ199-2]; MPUM 11445 [TJ199-3].

**Stratigraphic occurrence:** TJ193, TJ195, TJ199 from the Gundara Formation.

**Diagnosis:** Species of *Hemileurus* characterized by few and delayed ribs, 2-3 on the fold, 3-4 in the sulcus and 3 to 4 on each flank. Dorsal valve smoother than the ventral valve.

**Description:** Small biconvex shell; subovate to subpentagonal outline; maximum width: 4.5–7.0 mm, corresponding length: 5.5–7.1 mm; thickness variable from 2.9 to 5.7 mm. Fold and sulcus well defined; variably uniplicate anterior commissure. Ventral valve with straight umbo and moderately low interarea; delthyrium narrow with disjunct deltidial plates. Ornamentation of rounded delayed ribs numbering 2 to 3 ribs on the fold, 3 to 4 in the sulcus and 3 to 4 on each flank; growth lines imbricated near the anterior region. Ribs on the dorsal valve are weaker and more delayed.

Ventral valve interior with moderately short dental plates, closely set to the valve wall. Dorsal valve interior with divided hinge plate and curved crura.

**Discussion:** *Hemileurus politus* n. sp. differs from *Hemileurus runcinatus* Cooper and Grant, 1976 by its lower number of ribs and its smaller size. *Hemileurus orbicularis* Jin and Sun, 1981 appears to be larger than *H. politus* n. sp., having a width of 10.0

mm and a length of 9.3 mm and an L/W ratio usually less than 1.

This is the first occurrence of the genus *Hemileurus* in the Pamirs and the second in Asia. The other two species of the genus, *Hemileurus runcinatus* and *Hemileurus orbicularis* are from the Neal Ranch Formation, Texas (Cooper and Grant, 1976) and from the Kungurian Tunglonggongba Formation of Domar, Tibet (Jin and Sun, 1981), respectively.

Order ATHYRIDIDA Boucot, Johnson and Staton, 1964
Suborder ATHYRIDIDINA Boucot, Johnson and Staton, 1964
Superfamily ATHYRIDOIDEA Davidson, 1881
Family ATHYRIDIDAE Davidson, 1881
Subfamily SPIRIGERELLINAE Grunt, 1965

Genus *Posicomta* Grunt, 1986
**Type species:** *Posicomta gundarensis* Grunt, 1986.
**Remarks:** *Posicomta* Grunt, 1986 is very similar to *Composita* Brown, 1845 from which it differs by its smaller size and thicker shell substance. Another allied genus is *Spirigerella* Waagen, 1883, which differs by its complete foramen and its dental plates that are deeply buried in shell thickening.

*Posicomta gundarensis* Grunt, 1986
(Figs. 19, 22Ac-Bx)

1986 *Posicomta gundarensis* – Grunt, p. 120, pl. 16, figs. 9-13.

**Material:**
206 Articulated specimens: MPUM 11470 [TJ192 (9 specimens)]; MPUM 11523 [TJ193-1]; MPUM 11449 [TJ193-2]; MPUM 11450 [TJ193-3]; MPUM 11471 [TJ193 (37 specimens)]; MPUM 11451 [TJ194-1]; MPUM 11452 [TJ194-2]; MPUM 11453 [TJ194-3]; MPUM 11454 [TJ194-4]; MPUM 11472 [TJ194 (52 specimens)]; MPUM 11455 [TJ195-1]; MPUM 11456 [TJ195-2]; MPUM 11457 [TJ195-3]; MPUM 11458 [TJ195-4]; MPUM 11459 [TJ195-5]; MPUM 11473 [TJ195 (14 specimens)]; MPUM 11461 [TJ197-2]; MPUM 11462 [TJ197-3]; MPUM 11463 [TJ197-4]; MPUM 11474 [TJ197 (17 specimens)]; MPUM 11465 [TJ198-2]; MPUM 11466 [TJ198-3]; MPUM

11467 [TJ198-4]; MPUM 11469 [TJ198-6]; MPUM 11475 [TJ198 (47 specimens)]; MPUM 11476 [TJ199 (11 specimens)].

26 Ventral valves: MPUM 11470 [TJ192 (6 specimens)]; MPUM 11471 [TJ193 (5 specimens)]; MPUM 11472 [TJ194-1 (2 specimens)]; MPUM 11473 [TJ195-14 (2 specimens)]; MPUM 11460 [TJ197-1]; MPUM 11474 [TJ197 (3 specimens)]; MPUM 11468 [TJ198-5]; MPUM 11475 [TJ198 (2 specimens)]; MPUM 11476 [TJ199 (4 specimens)].

15 Dorsal valve: MPUM 11470 [TJ192]; MPUM 11471 [TJ193 (5 specimens)]; MPUM 11472 [TJ194]; MPUM 11473 [TJ195 (2 specimens)]; MPUM 11474 [TJ197 (2 specimens)]; MPUM 11464 [TJ198-1]; MPUM 11475 [TJ198 (3 specimens)].

14 Fragments: MPUM 11470 [TJ192 (2 specimens)]; MPUM 11472 [TJ194 (10 specimens)]; MPUM 11473 [TJ195 (2 specimens)].

Figured specimens: MPUM 11523 [TJ193-1]; MPUM 11449[TJ193-2]; MPUM 11450 [TJ193-3]; MPUM 11451 [TJ194-1]; MPUM 11452 [TJ194-2]; MPUM 11453 [TJ194-3]; MPUM 11454 [TJ194-4]; MPUM 11455 [TJ195-1]; MPUM 11456 [TJ195-2]; MPUM 11457 [TJ195-3]; MPUM 11458 [TJ195-4]; MPUM 11459 [TJ195-5]; MPUM 11460 [TJ197-1]; MPUM 11461[TJ197-2]; MPUM 11462 [TJ197-3]; MPUM 11463 [TJ197-4]; MPUM 11464 [TJ198-1]; MPUM 11465 [TJ198-2]; MPUM 11466 [TJ198-3]; MPUM 11467 [TJ198-4]; MPUM 11468 [TJ198-5]; MPUM 11469 [TJ198-6].

**Stratigraphic occurrence:** TJ192, TJ193, TJ194, TJ195, TJ197, TJ198, TJ199 from the Gundara Formation.

**Description:** *Posicomta gundarensis* comprises two morphotypes, worth to be described separately.

Morphotype A (L/W ratio > 1.27, high interarea): Small sized, strongly biconvex shell in either juveniles and adults; outline subovate with maximum width: 4.6–10.6 mm, corresponding length: 6.2–16.0 mm, L/W ratio > 1.27; shell substance moderately thick in the posterior region; anterior commissure distinctly uniplicate; ventral umbo slender with a subcircular to subelliptical foramen interrupted by a delthyrium with very narrow deltidial plates; interarea rather high and distinct; ventral sulcus narrow but variable in depth, from nearly absent to well developed; shell surface with variably expressed growth lamellae.

Ventral valve interior with distinct dental plates. Dorsal valve interior with a very well developed cardinal plate with two cardinal flanges; hinge plate medially

depressed; dorsal foramen in juveniles, absent in adults.

Morphotype B (L/W ratio < 1.27, low interarea): Small sized, biconvex to strongly biconvex shell in either juveniles and adults; outline subpentagonal to subovate with maximum width: 4.9–11.5 mm, corresponding length: 5.7–13.6 mm, L/W ratio < 1.27; shell substance moderately thick in the posterior region; anterior commissure rectimarginate to uniplicate. Ventral umbo short with a subcircular foramen interrupted by a delthyrium with very narrow deltidial plates; interarea low; delthyrium concealed by the dorsal umbo; ventral sulcus absent to moderately developed; shell surface with variably expressed growth lamellae.

Ventral valve interior with distinct dental plates. Dorsal valve interior with a very well developed cardinal plate with two cardinal flanges; hinge plate medially depressed; dorsal foramen in juveniles, absent in adults.

**Discussion:** *Posicomta gundarensis* Grunt, 1986 was erected to include specimens collected in the Gundara Formation of the Gundara valley. Based on the study of our collection, which is made of topotypes, we conclude that it contains two morphotypes that differ in their outline and the height of the interarea. In particular, they have a different L/W ratio (Fig. 19) which allows morphotype A (L/W ratio > 1.27) (Fig. 22Ai-Ak) to have a more elongated outline. The outline of morphotype B (Fig. 22Al-Ap) is more subovate or subpentagonal; also its interarea seems to be lower. If this can be interpreted as a sexual variation, it is hard to support.

An allied species from the North Pamir is *Posicomta zaalaica* Grunt, 1986 which is characterized by a larger size, a lower ventral umbo and less distinct fold and sulcus. *Posicomta dolabrata* (Grant, 1976) from the Guadalupian of Ko Muk, Thailand, has a very different outline and a foramen that appears larger if we consider the proportions of the shell. It is also smaller compared to *Posicomta gundarensis. Posicomta advena* (Grant, 1976), also from the Guadalupian of Ko Muk, Thailand, seems to be similar in size and outline to *Posicomta gundarensis*, but its commissure is more strongly uniplicate. *Posicomta subsolana* (Grant, 1976), from the Guadalupian of Khao Chang and Ban Kao, Thailand, is larger than *Posicomta gundarensis* and it has a delayed fold and a more strongly uniplicate anterior commissure.

Order SPIRIFERIDA Waagen, 1883

Suborder SPIRIFERIDINA Waagen, 1883

Superfamily AMBOCOELIOIDEA George, 1931

Family AMBOCOELIIDAE George, 1931

Genus *Orbicoelia* Waterhouse and Piyasin, 1970

**Type species:** *Orbicoelia fraterculus* Waterhouse and Piyasin, 1970.

**Remarks:** *Orbicoelia* Waterhouse and Piyasin, 1970 differs from the allied genus *Crurithyris* George, 1931 because of its narrower umbo, higher interarea, and rectimarginate commissure. Also, *Crurithyris* has weak sulci in both valves producing an emarginated commissure and a micrornamentation of fine spinules of two size. Another allied genus, *Cruricella* Grant, 1976 is remarkably smaller and it has more angular cardinal extremities, a wider interarea, a flatter dorsal valve and a maximum width that is more anteriorly located than *Orbicoelia*.

*Orbicoelia* sp. indet.

(Fig. 23A-N)

**Material:**

23 Articulated specimens: MPUM 11477 [TJ192-2]; MPUM 11478 [TJ192-3]; MPUM 11479 [TJ192-4]; MPUM 11480 [TJ192 (15 specimens)]; MPUM 11481 [TJ193 (5 specimens)].

3 Fragments: MPUM 11480 [TJ192 (3 specimens)].

Figured specimens: MPUM 11477 [TJ192-2]; MPUM 11478 [TJ192-3]; MPUM 11479 [TJ192-4].

**Stratigraphic occurrence:** TJ192, TJ193 from the Gundara Formation.

**Description:** Small to medium size, unequally biconvex shell with subovate to subpentagonal outline; cardinal extremities rounded; maximum width: 4.3–9.0 mm, anterior to the cardinal margin, corresponding length: 4.0–8.2 mm; anterior commissure from rectimarginate to broadly uniplicate; fold and sulcus absent. Ventral valve convex with high apsacline interarea; delthyrium open, moderately wide and high. Dorsal valve much less convex than the ventral one with subcircular outline; Shell surface smooth with evident silicification rings.

Ventral valve interior with teeth supported by dental ridges without dental plates.

**Discussion:** The specimens under examination differ from *Orbicoelia fraterculus* by a more convex dorsal valve and a less recurved and wider ventral interarea.

Superfamily Spiriferoidea King, 1846
Family Spiriferidae King, 1846
Subfamily Spiriferinae King, 1846

Genus *Larispirifer* Enokjan and Poletaev, 1986
**Type species:** *Choristites jigulensis riphaeicus* Aleksandrov and Einor in Einor, 1979.
**Remarks:** The genus *Larispirifer* Enokjan and Poletaev, 1986 has been discussed by Poletaev (1986), Shi and Waterhouse (1996) and Angiolini and Stephenson (2008). It is similar to *Purdonella* Reed, 1944 but it has a much wider hinge and broader ribs. *Larispirifer* occurs in the upper Pennsylvanian of the Russian Platform, in the Asselian of northern Timan, in the Sakmarian–Artinskian of northern Yukon (Canada) (Shi and Waterhouse, 1996) and in the Asselian of N Iran (Angiolini and Stephenson, 2008).

*Larispirifer* sp. indet.
(Fig. 24)

**Material:**
6 ventral valves: MPUM 11482 [TJ181-1]; MPUM 11483 [TJ181-2]; MPUM 11484 [TJ181-3]; MPUM 11485 [TJ181-4]; MPUM 11486 [TJ181 (2 specimens)].
Several fragments: MPUM 11486 [TJ181].
Figured specimens: MPUM 11482 [TJ181-1]; MPUM 11483 [TJ181-2]; MPUM 11484 [TJ181-3]; MPUM 11485 [TJ181-4].
**Stratigraphic occurrence:** TJ181 from the Safetdara Formation.
**Description:** Large sized, convex ventral valve, with transverse subrectangular outline. Maximum width > 100 mm anterior to the hinge; corresponding length > 90 mm. Cardinal extremities can be subangular (90°). Shell substance very thick.

Ventral interarea trapezoidal, denticulate. Ventral sulcus shallow, "V" shaped, posteriorly narrower and deeper but widening and shallowing anteriorly, ornamented by about 8-10 ribs. Ornamentation of flanks with flat, unequal, bifurcating ribs, numbering 7-8 per 5 mm near the umbo and 2 per 5 mm at the anterior margin; growth lines and lamellae occur anteriorly.

Interior of ventral valve with thick, dental plates buried apically in the shell thickening and slightly divergent anteriorly.

**Discussion:** Although represented by a few broken ventral valves, this species is remarkable for its size, shell thickness and ornamentation which, along with the internal characters, permit assignment to the genus *Larispirifer*. The specimens from the Safetdara Formation differ from *L. riphaeicus* (Aleksandrov and Einor in Einor, 1979) and from *L. ettrainensis* Shi and Waterhouse, 1996 by their larger size, shallower sulcus, posteriorly finer ribs and cardinal extremities at 90°C. They also differ from *Larispirifer fantinisestinii* Angiolini in Angiolini and Stephenson, 2008 because of their larger size, thicker shell substance, less transverse outline and coarser and flatter ribs anteriorly.

The occurrence of a species of *Larispirifer* in the Kungurian Safetdara Formation is the youngest record for the genus, which is known from the upper Pennsylvanian to the Artinskian.

Order SPIRIFERINIDA Ivanova, 1972
Suborder SPIRIFERINIDINA Ivanova, 1972
Superfamily PENNOSPIRIFERINOIDEA Dagys, 1972
Family SPIRIFERELLINIDAE Ivanova, 1972

Genus *Spiriferellina* Frederiks, 1924
**Type species:** *Terebratulites cristatus* von Schlotheim, 1816.

*Spiriferellina* sp. indet.
(Fig. 23O-Z)

**Material:**
7 Articulated specimens: MPUM 11490 [TJ192 (2 specimens)]; MPUM 11491 [TJ193]; MPUM 11492 [TJ194]; MPUM 11493 [TJ195 (2 specimens)]; MPUM 11488 [TJ199-7].
4 Ventral valves: MPUM 11490 [TJ192]; MPUM 11487 [TJ193-5]; MPUM 11489 [TJ199-8]; MPUM 11494 [TJ199].
2 Dorsal valves: MPUM 11490 [TJ192 (2 specimens)].
4 Fragments: MPUM 11494 [TJ199 (4 specimens)].
Figured specimens: MPUM 11487 [TJ193-5]; MPUM 11488 [TJ199-7]; MPUM 11489 [TJ199-8].

**Stratigraphic occurrence:** TJ192, TJ193, TJ194, TJ195, TJ199 from the Gundara Formation.

**Description:** Medium sized biconvex shell with subtrigonal outline; maximum width: 8.2–20.0 mm, corresponding length: 7.8–18 mm; cardinal extremites rounded; anterior commissure uniplicate; shell substance punctate. Ventral valve with moderately high and apsacline interarea; well defined sulcus, wider than the intercostal furrows and flat bottomed. Dorsal valve with orthocline interarea and well defined fold. Ornamentation of 5 to 6 moderately rounded ribs on each flank with deep intercostal furrows; growth laminae well developed and imbricated anteriorly.

Ventral valve interior with dental plates with moderately short adminicula. Dorsal valve interior with cardinal process (ctenophoridium), sockets delimited by sockets ridges; moderately broad crural bases.

**Discussion:** The examined specimens are similar in size and shell shape to *Spiriferellina cristata* (von Schlotheim, 1816) from the Lopingian of Germany. The most significant difference is related to the ribs that, in the studied specimens, are rounded at the top and not flattened like what they appear in *Spiriferellina cristata.*

*Spiriferellina hilli* Girty, 1909 from the Word Formation, Texas, is smaller and the same can be said for *Spiriferellina nasuta* Cooper and Grant, 1976 from the Neal Ranch Formation, Texas, which can be further distinguished by its conical ventral valve. *Spiriferellina nuda* Cooper and Grant, 1976 from the Bell Canyon Formation, Texas, has a different outline and size and fewer plication on each flank. *Spiriferellina paucicostata* Cooper and Grant, 1976 from the Word Formation is similar in size, but differs in the cardinal extremities which are angular and also in the number of ribs which are fewer compared to the studied specimens. *Spiriferellina tricosa* Cooper and Grant, 1976 from the Cathedral Mountain Formation, Texas, is smaller and has weaker ribs than the studied specimens.

*Spiriferellina yanagidai* Grant, 1976 from the Guadalupian of Ko Muk, Thailand, is remarkably smaller and has fewer ribs than the studied specimens.

The specimens under exam are left in open nomenclature due to their poor state of preservation.

Family PARASPIRIFERINIDAE Cooper and Grant, 1976

Genus *Paraspiriferina* Reed, 1944

**Type species:** *Paraspiriferina ghundiensis* Reed, 1944.

**Remarks:** *Paraspiriferina* Reed, 1944 and *Callispirina* Cooper and Muir-Wood, 1951 are two very similar genera, but *Paraspiriferina* can be distinguished for being smaller with a better differentiated fold and sulcus. *Spiriferellina* Frederiks, 1924, which has a similar shape and outline, has fewer ribs on the flanks.

*Paraspiriferina* sp. indet.

(Fig. 23Aa-Ak)

**Material:**

2 Articulated specimens: MPUM 11495 [TJ195-12]; MPUM 11498 [TJ195].

1 Ventral valve: MPUM 11497 [TJ199-6].

1 Dorsal valve: MPUM 11496 [TJ199-5].

Figured specimens: MPUM 11495 [TJ195-12]; MPUM 11496 [TJ199-5]; MPUM 11497 [TJ199-6].

**Stratigraphic occurrence:** TJ195 and TJ199 from the Gundara Formation.

**Description:** Small and strongly biconvex shell with a subtrigonal to rhombic outline; maximum width: 4.4–5.5 mm, corresponding length: 4.2–5.5 mm; anterior commissure uniplicate; shell substance punctate. Ventral valve strongly convex with high apsacline to catacline relatively high interarea; sulcus well defined. Dorsal valve convex with nearly orthocline interarea; fold pretty well differentiated and slighty larger than ribs. Ornamentation of 3-4 rounded ribs with deep intercostal furrows on each flank and 2 to 3 ribs on the fold; growth lines imbricated anteriorly.

**Discussion:** The specimens under exam are similar in size and outline to *Paraspiriferina amoena* Cooper and Grant, 1976 from the Neal Ranch Formation, Texas, but they have a better defined sulcus, a higher interarea and stronger growth lines. *Paraspiriferina ghundiensis* Reed, 1944 from the Guadalupian of Salt Range, Pakistan, has a different outline, and a wider and larger fold. *Paraspiriferina billingsi* Shumard, 1859 from the Bell Canyon Formation and Capitan Formation of Texas is larger than the specimens under study, with a different outline and more plications for each flank; the same can be said for *Paraspiriferina evax* Girty, 1909 from the Bell Canyon Formation and the Capitan Formation. *Paraspiriferina gentilis* Grant, 1976 from Ko Muk, Thailand has fewer ribs and a deeper sulcus.

The specimens under exam are left in open nomenclature due to their poor state

of preservation.

Order TEREBRATULIDA Waagen, 1883
Suborder TEREBRATULIDINA Waagen, 1883
Superfamily DIELASMATOIDEA Schuchert, 1913
Family PSEUDODIELASMATIDAE Cooper and Grant, 1976

Genus *Fredericksolasma* Smirnova, 2001
**Type species:** *Hemiptychina pseudoelongata* var. *lata* Licharew, 1939.
**Remarks:** *Fredericksolasma* Smirnova, 2001 differs from *Pseudodielasma* Brill, 1940 and *Pleurolasma* Cooper and Grant, 1976 because it has an equibiconvex shell and it is characterized by the presence of an outer hinge plate. *Gundarolasmina* Smirnova and Grunt, 2003 has a different shell outline, it is larger and unequally biconvex; furthermore, *Gundarolasmina* has different dorsal internal characters, such as crural plates joined to the bottom of the dorsal valve, a ring-shaped loop and loop branches that are not differentiated from the crural plates and the crural bases.

*Levenolasma* Smirnova and Grunt, 2003 is distinguishable by its rooflike dorsal valve fitting into a flattened ventral valve, a long sulcus and a multiplicate commissure. The genus *Pyandzhelasma* Smirnova and Grunt, 2002 is much larger compared to *Fredericksolasma*, has a more defined sulcus, and a septalium formed by inner hinge plates resting on the valve floor.

*Heterelasmina* Licharew, 1939 even if similar in size, differs for two or three folds that are present anteriorly and for having a flatter dorsal valve.

*Rostranteris* Gemmellaro, 1899 is remarkably different, being characterized by a thick, multiplicate shell and different internal characters such as the presence of an inner hinge plate.

*Fredericksolasma lata* (Licharew, 1939)
(Fig. 23Al-Bk)

1939 *Hemiptychina pseudoelongata* var. *lata* – Licharew, p. 119, pl. 29, fig. 7.
2001 *Fredericksolasma lata* – Smirnova, text-figs. 7-10.
2007 *Fredericksolasma lata* – Smirnova, p, 806, pl. 5, figs. 11, 12.

**Material:**

44 Articulated specimens: MPUM 11508 [TJ193]; MPUM 11499 [TJ195-13]; MPUM 11509 [TJ195 (2 specimens)]; MPUM 11500 [TJ197-5]; MPUM 11510 [TJ197 (9 specimens)]; MPUM 11501 [TJ198-7]; MPUM 11503 [TJ198-13]; MPUM 11504 [TJ198-15]; MPUM 11511 [TJ198 (20 specimens)]; MPUM 11505 [TJ199-9]; MPUM 11506 [TJ199-11]; MPUM 11507 [TJ199-12]; MPUM 11512 [TJ199 (4 specimens)].

3 Ventral valves: MPUM 11510 [TJ197]; MPUM 11502 [TJ198-10]; MPUM 11511 [TJ198].

1 Dorsal valve: MPUM 11510 [TJ197].

Figured specimens: MPUM 11499 [TJ195-13]; MPUM 11500 [TJ197-5]; MPUM 11501 [TJ198-7]; MPUM 11502 [TJ198-10]; MPUM 11503 [TJ198-13]; MPUM 11504 [TJ198-15]; MPUM 11505 [TJ199-9]; MPUM 11506 [TJ199-11]; MPUM 11507 [TJ199-12].

**Stratigraphic occurrence:** TJ193, TJ195, TJ197, TJ198, TJ199 from the Gundara Formation.

**Description:** Equally biconvex shell with subovate outline; maximum convexity near the umbo, anterior region flat; maximum width: 4.6–8.9 mm at midlength, corresponding length: 5.7–11.4 mm; anterior commissure mostly rectimarginate, more rarely weakly uniplicate; lateral commissure slightly to moderately arched. Ventral umbo wide, highly curved and high with well-defined and circular foramen; sulcus rarely present and very shallow. Dorsal fold absent.

Ventral valve interior with pedicle collar. Dorsal valve interior with moderately large crura; narrow loop flanges; transverse band directed upward and curved in the middle; outer hinge plate separated; inner hinge plate absent.

**Discussion:** *Fredericksolasma lata* (Licharew, 1939) differs from *Fredericksolasma rhomboidalis* Smirnova and Grunt, 2003 in its wider and rounded outline, its less convex dorsal valve and the occurrence of a pedicle collar. *Fredericksolasma lata* differs from *Fredericksolasma darvasica* (Tschernyschew, 1914) in its rounded outline, its less defined sulcus, a less developed outer hinge plate and a differently shaped transverse band of the loop.

*Fredericksolasma lata* differs from *Fredericksolasma nummulus* (Waagen, 1882) in the smaller size of the shell, its equiconvex valves, and the curved lateral commissure; it differs from *Fredericksolasma sublaevis* (Waagen, 1882) by its

equiconvex valves and wider umbo.

*Fredericksolasma rhomboidalis* Smirnova and Grunt, 2003
(Fig. 23Bl-Bu)

1914 *Hemiptychina* (*Beecheria*) *pseudoelongata* – Tschernyschew, p. 8, pl. 2, figs. 14-17.
2003 *Fredericksolasma rhomboidale* – Smirnova and Grunt, p. 35, text-figs. 1i-1n, 3.
2007 *Fredericksolasma rhomboidale* – Smirnova, p. 806, pl. 5, fig. 13.

**Material:**
12 Articulated specimens: MPUM 11516 [TJ195 (2 specimens)]; MPUM 11517 [TJ197 (2 specimens)]; MPUM 11513 [TJ198-9]; MPUM 11514 [TJ198-14]; MPUM 11518 [TJ198 (2 specimens)]; MPUM 11515 [TJ199-10]; MPUM 11519 [TJ199 (3 specimens)].
Figured specimens: MPUM 11513 [TJ198-9]; MPUM 11514 [TJ198-14]; MPUM 11515 [TJ199-10].
**Stratigraphic occurrence:** TJ195, TJ197, TJ198, TJ199 from the Gundara Formation.
**Description:** Equibiconvex shell with suboval to tear-shaped outline; maximum convexity near the umbo, anterior region flat; maximum width: 5.4–7.3 mm anterior to mid-length, corresponding length: 7.4–8.9 mm; anterior commissure mostly rectimarginate, rarely weakly uniplicate; lateral commissure slightly to moderately arched. Ventral umbo wide, highly curved and high with well defined and circular foramen; sulcus rarely present and very shallow. Dorsal fold absent.

Ventral valve interior without pedicle collar. Dorsal valve interior with moderately large crura; narrow loop flanges; transverse band directed upward and curved in the middle; outer hinge plate separated; inner hinge plate absent.
**Discussion:** Erected as *Fredericksolasma rhomboidale*, its specific name has been corrected here to *Fredericksolasma rhomboidalis* because the adjective ending should be feminine in Latin and thus *–is* not *–e*.

This species differs from the other species of the genus by its tear-shaped, subrhombic outline and by the absence of a pedicle collar.
**Other occurrences:** *Fredericksolasma rhomboidalis* occurs also in the Chapsai Formation of southwestern Darvaz.

*Fredericksolasma* sp. indet.
(Fig. 23Bv, Bw)

**Material:**
6 Fragments: MPUM 11522 [TJ192 (4 specimens)]; MPUM 11520 [TJ198-11]; MPUM 11521 [TJ198-12].
Figured specimens: MPUM 11520 [TJ198-11]; MPUM 11521 [TJ198-12].
**Stratigraphic occurrence:** TJ192, TJ198 from the Gundara Formation.
**Remarks:** The incomplete state of preservation of these specimens prevent a specific assignment. However, they show some interesting internal features which are important for the definition of the genus and so they are figured herein.

**Acknowledgments**
LA and AZ were supported by DARIUS PROGRAMME, Project CA11/01. V. Minaev and E. Kanaev, are thanked for field assistance in the Pamirs and for permissions. Two anonymous reviewers are thanked for their constructive comments. Giovanni Chiodi, Curzio Malinverno and Agostino Rizzi are acknowledged for technical support.

**References** (author of species and that of higher taxonomic categories are not included)

Angiolini, L., Stephenson, M.H., 2008. Lower Permian brachiopods and palynomorphs from the Dorud Formation (Alborz Mountains, north Iran): new evidence for their palaeobiogeographic affinity. Fossils and Strata 54, 117-132.

Angiolini, L., Zanchi, A., Zanchetta, S., Nicora, A., Vezzoli, G., 2013. The Cimmerian geopuzzle: new data from South Pamir. Terra Nova 25, 352-360.

Angiolini, L., Zanchi, A., Zanchetta, S., Nicora, A., Vuolo, I., Berra, F., Henderson, C., Malaspina, N., Rettori, R., Vachard, D., Vezzoli, G., 2015. From rift to drift in South Pamir (Tajikistan): Permian evolution of a Cimmerian terrane. Journal of Asian Earth Sciences 102, 146-169.

Burtman, V.S., Molnar, P., 1993. Geological and geophysical evidence for deep subduction of continental crust beneath the Pamir. Special Papers — Geological Society of America 281, 1-76.

Chernykh, V.V., 2006. Lower Permian Conodonts in the Urals [Nizhnepermskie konodonti Urala]. Institute of Geology and Geochemistry, Uralian Branch of the Russian Academy of Sciences, Ekaterinburg, 130 pp. (in Russian).

Cooper, G.A., Grant, R.E., 1976. Permian Brachiopods of west Texas IV. Smithsonian Contributions to Paleobiology 21, 1923-2608.

Davydov, V.I., Krainer, K., Chernykh, V., 2013. Fusulinid biostratigraphy of the Lower Permian Zweikofel Formation (Rattendorf Group; Carnic Alps, Austria) and Lower Permian Tethyan chronostratigraphy. Geological Journal 48, 57-100.

Deprat, J., 1915. Etude des Fusulinidés de Chine et d'Indochine et classification des calcaires à Fusulines. (IVe Mémoire), les Fusulinidés des calcaires Carbonifériens et Permiens du Tonkin, du Laos et du Nord-Annam. Service Géologique de l'Indochine, Mémoire 4 (1), 1-30.

Dronov, V.L., Leven, E.Ya., 1990. Age of carbonate conglomerates of the central zone of SE Pamir. Doklady Akademi Nauk Tadjik SSR 25, 232-235 (in Russian).

Filimonova, T.V., 2008. Smaller foraminifers from type sections of the Bolorian Stage, the Lower Permian of Darvaz. Stratigraphy and Geological Correlation 16 (6), 599-617.

Grant, R.E., 1976. Permian brachiopods from southern Thailand. Journal of Paleontology 50 (Supplement to No. 3, Paleontological Society Memoir 9), 1-269.

Grunt, T.A., 1986. Classification of brachiopods of the Order Athyridida. Akademii Nauk SSSR, Trudy Paleontologischeskogo Instituta 215, 1-200 (in Russian).

Hamburger, M.W., Sarewitz, D.R., Pavlis, T.L., Popandopulo, G.A., 1992. Structural and seismic evidence for intracontinental subduction in the Peter the First Range, Central Asia. Geological Society America Bulletin 104, 397-408.

Jin, Y., Sun, D., 1981. Palaeozoic brachiopods from Xizang. In: Nanjing Institute of Geology and Palaeontology (Ed.), Palaeontology of Xizang, Book III (The Series of the Scientific Expedition to the Qinghai-Xizang Plateau). Science Press, Beijing, pp. 127-176 (in Chinese).

Kobayashi, F., 2005. Permian foraminifers from the Itsukaichi-Ome area, West Tokyo, Japan. Journal of Paleontology 79 (3), 413-432.

Leven, E.Ya., 1963. On the phylogeny of advanced fusulinids and subdivision of Tethyan Late Permian deposits. Voprosy Mikropaleontologii 7, 57-70 (in Russian).

Leven, E.Ya., 1967. Stratigraphy and Fusulinids of Permian Deposits of Pamirs. Transaction of Geological Institute of Academy of Science of USSR 167, 224 pp. (in Russian).

Leven E.Ya., 1979. Bolorian Stage of the Permian: Substantiation, Characteristics, Correlation. Izvestiya Akademii Nauk SSSR Seriya Geologicheskikh 1, 53-65 (in Russian).

Leven, E.Ya., 1980. Explanatory notes for the Stratigraphic Scale of Permian deposits of the Tethyan Region. Transactions of VSEGEI, 3-51 (in Russian).

Leven, E.Ya., 1981. The late Paleozoic from Charymdary, Gundara and Zidadar rivers in southeastern Darvaz. Byulleten Moskovskogo Obshchestva Ispytatelei Prirody 56 (4), 40-52 (in Russian).

Leven, E.Ya., 1997. Permian stratigraphy and Fusulinida of Afghanistan with their paleogeographic and paleotectonic implications. In: Stevens, C.H., Baars, D.L. (Eds.), Permian Stratigraphy and Fusulinida of Afghanistan with Their Paleogeographic and Paleotectonic Implications. Geological Society of America Special Papers 316, pp. 1-134.

Leven, E.Ya., 1998. Permian fusulinids assemblages and stratigraphy of Transcaucasia. Rivista Italiana di Paleontologia e Stratigrafia 104 (3), 299-328.

Leven, E.Ya., 2001. On possibility of using the Global Permian Stage Scale in the Tethyan Region. Stratigraphy and Geological Correlation 9 (6), 118-131.

Leven, E.Ya., 2012. The Bashkirian Stage of Southwestern Darvaz, the Pamir Mountains: Stratigraphy and Paleotectonics. Stratigraphy and Geological Correlation 20 (3), 240-260.

Leven, E.Ya., Bogoslovskaya, M.F., 2006. The Roadian stage of the Permian and problems of its global correlation. Stratigraphy and Geological Correlation 14 (2), 164-173.

Leven, E.Ya., Shcherbovich, S.F., 1978. Fusulinids and Stratigraphy of the Asselian Stage in Darvaz. Nauka, Moscow, 162 pp. (in Russian).

Leven, E.Ya., Shcherbovich, S.F., 1980. Fusulinid assemblages of the Darvaz Sakmarian Stage. Voprosy Micropaleontologii 23, 71-85 (in Russian).

Leven, E.Ya., Grunt, T.A., Dmitriev, V.Y., 1983. Bolorian stage of the Permian: Type Sections. Izvestiya Akademii Nauk SSSR Seriya Geologicheskikh 8, 35-45 (in Russian).

Leven, E.Ya., Leonova T.B., Dmitriev, V.Y., 1992. Permian of the Darvaz-Transalay Zone of Pamirs: Fusulinids, Ammonoids, Stratigraphy. Transactions of Paleontological Institute of Russian Academy of Sciences 253, 1-197 (in Russian).

Licharew, B.K., 1939. Class Brachiopoda. Atlas of the Index Forms of the Fossil Faunas of the USSR, Vol. 7: The Permian System. Tsentr Nauchno-lssledovatelskogo Geologorazved Instituta, Moscow-Leningrad, pp. 76-121 (in Russian).

Lys, M., 1994. Les Fusulinida d'Asie orientate de'crits par J. Deprat. Revision et mise en valeur de la collection-type. Cahiers de Micropaleontologie 9 (1), 1-57.

Miklukho-Maklay, A.D., 1958. On Stage subdivision on marine Permian deposits of the USSR southern regions. Doklady Akademii Nauk SSSR 120, 175-178 (in Russian).

Perez-Huerta, A., Sheldon, N.D., 2006. Pennsylvanian sea level cycles, nutrient availability and brachiopod paleoecology. Palaeogeography, Palaeoclimatology, Palaeoecology 230, 264-279.

Poletaev, S.V., 1986. Choristitid brachiopods of the Family Spiriferidae. Paleontological Journal 20, 54-64.

Reiter, K., Kukowski, N., Ratschbacher, L., 2011. The interaction of two indenters in analogue experiments and implications for curved fold-and-thrust belts. Earth and Planetary Science Letters 302, 132-146.

Riding, R., 2002. Structure and composition of organic reefs and carbonate mud mounds: concepts and categories. Earth-Science Reviews 58, 163-231.

Robinson, A.C., 2015. Mesozoic tectonics of the Gondwanan terranes of the Pamir plateau. Journal of Asian Earth Science 102, 170-179.

Robinson, A.C., Ducea, M., Lapen, T.J., 2012. Detrital zircon and isotopic constraints on the crustal architecture and tectonic evolution of the northeastern Pamir. Tectonics 31, TC2016, doi: 10.1029/2011TC003013.

Rozovskaya, S.E., 1975. Sostav, sistema i filogeniya otryada fuzulinida (Composition, phylogénie et systématique de l'ordre des Fusulinida). Akademiya Nauk SSSR, Trudy Paleontologischeskogo Instituta 149, 1-267 (in Russian).

Ruzhentsev, V.E., 1954. The Asselian Stage of the Permian System. Dokl Akad Nauk SSSR 99 (6), 1079-1082 (in Russian).

Ruzhentsev, S.V., Shol'man, V.A., 1982. Tectonic zoning of the Pamirs and Afghanistan. In: Sinha, A.K. (Ed.), Contemporary Geoscientific Researches in Himalaya. Dehra Dun, India, pp. 53-59.

Ruzhentsev, S.V., Pospelov, I.I., Sukhov, A.N., 1977. Tectonics of the Kalaikhumb-Sauksay Zone of North Pamir. Geotektonika 4, 68-79.

Schwab, M., Ratschbacher, L., Siebel, W., McWilliams, M., Minaev, V., Lutkov, V., Chen, F., Stanek, K., Nelson, B., Frisch, W., Wooden, J.L., 2004. Assembly of the Pamirs: Age and origin of magmatic belts from the southern Tien Shan to the southern Pamirs and their relation to Tibet. Tectonics 23, TC4002, doi: 10.1029/2003TC001583.

Shen, S.Z., Yuan, D.Z., Henderson, C.M., Tazawa, J., Zhang, Y.C., 2013. Implications of Kungurian (Early Permian) conodonts from Hatahoko, Japan, for correlation between the Tethyan and international timescales. Micropaleontology 58 (6), 505-522.

Shi, G.R., Waterhouse, J.B., 1996. Lower Permian brachiopods and molluscs from the upper Jungle Creek Formation, northern Yukon Territory, Canada. Geological Survey of Canada Bulletin 424, 241 pp.

Smirnova, T.N., 2001. Systematics and phylogeny of the Late Permian Terebratulids (Brachiopoda) from Darvaz. Paleontological Journal 35 (2), 140-151.

Smirnova, T.N., 2007. Permian Terebratulids of Eurasia: morphology, systematics, and phylogeny. Paleontological Journal 41 (7), 707-813.

Smirnova, T.N., Grunt, T.A., 2003. New Permian Brachiopods of the Order Terebratulida from the Southwestern Darvaz (Northern Pamirs). Paleontological Journal 37 (2), 138-144.

Tschernyschew, F.N., 1914. Fauna of the Upper Paleozoic Deposits of the Darvaz Ridge. Trudy Geologicheskago Komiteta, New Series 104, 1-66 (in Russian).

Ueno, K., 1991a. *Pamirina* (Permian Fusulinacea) from the Akiyoshi Limestone Group, Southwest Japan. Transactions and Proceedings of the Palaeontological Society of Japan 161, 739-750.

Ueno, K., 1991b. Early evolution of the families Verbeekinidae and Neoschwagerinidae (Permian fusulinacea) in the Akiyoshi Limestone Group, southwest Japan. Transactions and Proceedings of the Palaeontological Society of Japan 164, 973-1002.

Ueno, K., 1996. Late early to middle Permian fusulinacean biostratigraphy of the Akiyoshi Limestone Group, southwest Japan, with special reference to the Verbeekinid and Neoschwagerinid fusulinacean biostratigraphy and evolution. Reports of Shallow Tethys 4, International Symposium Albrechtsberg, Austria, 1994. Annali dei Musei Civici di Rovereto, Sezione Archeologia, Storia e Scienze Naturali 11, 77-104.

Vachard, D., Vandelli, A., Moix, P., 2013. Discovery of the *Misellina* Zone (latest Kungurian) in the Lentas unit of the Pindos series (Crete). Geobios 46, 521-537.

Vlasov, N.G., Dyakov, Y.A., Cherev, E.S., 1991. Geological map of the Tajik SSR and adjacent territories, 1:500,000. VSEGEI (Vsesojuznoi Geologicheskiy Institut) Leningrad, Saint Petersburg.

Williams, A, Carlson, S.J., Brunton, C.H.C., Holmer, L.E., Popov, L.E., Mergl, M., Laurie, J.R., Bassett, M.G., Cocks, L.R.M., Rong, J.Y., Lazarev, S.S., Grant, R.E., Racheboeuf, P.R., Jin, Y.G., Wardlaw, B.R., Harper, D.A.T., Wright, A.D., 2000. Treatise on Invertebrate Paleontology. Part H, Brachiopoda (revised). Volumes 2 & 3, Linguliformea, Craniiformea, Rhynchonelliformea (part). The Geological Society of America and the University of Kansas Press, Boulder, Colorado and Lawrence, Kansas, pp. 1-919.

Williams, A., Brunton, C.H.C., Carlson, S.J., Alvarez, F., Blodgett, R.B., Boucot, A.J., Copper, P., Dagys, A.S., Grant, R.E., Jin, Y.G., MacKinnon, D.I., Mancenido, M.O., Owen, E.F., Rong, J.Y., Savage, N.M., Sun, D.L., 2002. Treatise on Invertebrate Paleontology. Part H, Brachiopoda (revised). Volume 4, Rhynchonelliformea (part). The Geological Society of America and the University of Kansas Press, Boulder, Colorado and Lawrence, Kansas, pp. 921-1688.

Williams, A., Brunton, C.H.C., Carlson, S.J., Carter, J.L., Curry, G.B., Dagys, A.S., Gourvennec, R., Hou, H.F., Jin, Y.G., Johnson, J.G., Lee, D.E., MacKinnon, D.I., Racheboeuf, P.R., Smirnova, T.N., Sun, D.L., 2006. Treatise on Invertebrate Paleontology. Part H, Brachiopoda (revised). Volume 5,

Rhynchonelliformea (part). The Geological Society of America and the University of Kansas Press, Boulder, Colorado and Lawrence, Kansas, pp. 1689-2320.

Williams, A., Brunton, C.H.C., Carlson, S.J., Alvarez, F., Baker, P.G., Bassett, M.G., Boucot, A.J., Carter, J.L., Cocks, L.R.M., Cohen, B.L., Curry, G.B., Cusack, M., Emig, C.C., Gourvennec, R., Harper, D.A.T., Holmer, L.E., Lee, D.E., Logan, A., Luter, D., MacKinnon, D.I., Mancenido, M.O., Mergl., M., 2007. Treatise on Invertebrate Paleontology. Part H, Brachiopoda (revised). Volume 6, Supplement. The Geological Society of America and the University of Kansas Press, Boulder, Colorado and Lawrence, Kansas, pp. 2321-2355.

Zhai, Q.G., Jahn, B.M., Wang, J., Hu, P.Y., Chung, S.L., Lee, H.Y., Tang, S.H., Tang, Y., 2016. Oldest Paleo-Tethyan ophiolitic mélange in the Tibetan Plateau. Geological Society of America Bulletin 128 (3-4), 355-373, doi: 10.1130/B31296.1.

Zhang, Y.C., Shen, S.Z., Zhai, Q.G., Zhang, Y.J., Yuan, D.X., 2015. Discovery of a *Sphaeroschwagerina* fusuline fauna from the Raggyorcaka Lake area, northern Tibet: implications for the origin of the Qiangtang metamorphic belt. Geological Magazine, Rapid Communication Online, 1-7, doi: 10.1017/S0016756815000795.

**Figure captions**

Fig. 1. Tectonic setting of Southeast Pamir, Central Pamir and North Pamir, located between the Eurasian plate to the north and the Karakorum, Kohistan/Ladakh and the Indian plate to the south. The study area is outlined in pink. KKSZ: Karakoram-Kohistan suture zone; MMT: Main mantle thrust; NCS: North Pamir-Central Pamir suture zone. Modified from Angiolini et al. (2013).

Fig. 2. Geological map of the study area based on Leven et al. (1983) and the 1:200,000 scale Russian maps of Tajikistan, showing the location of the stratigraphic logs.

Fig. 3. Stratigraphic scheme of the Permian formations of Darvaz based on data from Leven and Shcherbovich (1978), Leven (1981), Leven et al. (1983, 1992), and Leven (1997).

Fig. 4. Log of the Bolorian stratotype at the junction of the watersheds between the Charymdara, Zydadara and Gundara valleys (38°45'34''N, 70°53'27''E; 3420 m a.s.l. for the base of the section). The blank portions with oblique lines stand for covered strata. For the legend see Fig. 5.

Fig. 5. Log of Gundara section along the left side of the Gundara valley (38°45'45.1''N, 70°52'49.9''E; 3542 m a.s.l.). The blank portions with oblique lines stand for covered strata.

Fig. 6. Field photos showing the Bolorian stratotype section (above) and the Gundara section. Q.3835 indicates the elevation in metres above sea level.

Fig. 7. Representative photomicrographs of turiditic sandstones from Chelamchi Formation (A, B) and of fine sandstones from the Gundara Formation (C, D). Bt = biotite; Lv = volcanic grains; Pl = plagioclase; Q = quartz. Scale bar = 250 μm.

Fig. 8. Conodonts of the Safetdara Formation. Scale bar = 200 μm. (A-C) *Sweetognathus modulatus* Chernykh, 2006, upper, lateral and lower views, sample TJ163, Safetdara Formation, Bolorian Stratotype section, Tajikistan. (D-F) *Sweetognathus* sp., upper, lateral and lower views, sample TJ163, Safetdara Formation, Bolorian Stratotype section, Tajikistan. (G-I) *Sweetognathus* sp., upper, lateral and lower views, sample TJ163, Safetdara Formation, Bolorian Stratotype section, Tajikistan.

Fig. 9. Bolorian microfacies. Scale bar = 1 mm. (A) Bioclastic wackestone with *Leeina*? sp. (L), dasycladales *Connexia* sp. (Co) and *Mizzia yabei* (Karpinsky, 1908) (M), sample TJ171. (B) Bioclastic grainstone with two generations of cements (palissadic and drusy), of beach rock type, with *Leeina* ex gr. *fusiformis* (Schellwien in Schellwien and Dyhrenfurth, 1909) (L), *Brevaxina dyhrenfurthi* (Dutkevich in Likharev et al., 1939) (top left) (Br) and *Clavaporella* sp. 2 (bottom left) (Cl2),

sample TJ171. (C) Bioclastic wackestone passing to rudstone with *Leeina*? sp. (L), *Brevaxina dyhrenfurthi otai* (Sakaguchi and Sugano, 1966) emend. Ueno, 1991b (Br), *Agathammina*? sp. (Ag; see detail in Fig. 14C), and dasycladales *Mizzia cornuta* Kochansky-Devidé and Herak, 1960 (M), sample TJ163. (D) Bioclastic grainstone with two generations of cements (palissadic and drusy), of beach rock type, with *Brevaxina dyhrenfurthi* (Dutkevich in Likharev et al., 1939) (Br), *Darvasites* (Da), and *Palaeonubecularia* sp. (Pn), sample TJ171. (E, F) Bioclastic rudstone with diversified calcareous algae *Clavaporella* sp. 2 (Cl2), *Gyroporella* sp. (Gy), *Epimastopora* (Ep), *Mizzia* (M), phylloid algae (Ph), *Climacammina* sp. (Ca), *Neofusulinella pseudogiraudi* (Sheng, 1962 non 1963) (Np), *Leeina*? sp. (L), and *Brevaxina dyhrenfurthi* (Dutkevich in Likharev et al., 1939) (Br); (E) sample TJ179; (F) sample TJ179.

Fig. 10. Bolorian and Kubergandian microfacies. Scale bar = 1 mm. (A) Rudstone with *Darvasites* sp. (Da) (tangential subaxial section) and *Tubiphytes* sp. (T), sample TJ163. (B) Bioclastic rudstone with two generations of cements (palissadic and drusy), of beach rock type, with *Brevaxina* sp. (Br), *Leeina*? sp. (L), and *Darvasites* sp. (Da), sample TJ171. (C) Bioclastic rudstone (beach rocks) with *Brevaxina dyhrenfurthi* (Dutkevich in Likharev et al., 1939) (Br), phylloid algae (Ph), *Anthracoporella* sp. (An), *Leeina*? sp. (L), *Neofusulinella pseudogiraudi* (Sheng, 1962 non 1963) (Np), *Gyroporella* sp. (Gy) and *Tetrataxis* sp. (T), sample TJ170. (D) Bioclastic rudstone with two generations of cements (palissadic and drusy), of beach rock type, with *Brevaxina dyhrenfurthi* (Dutkevich in Likharev et al., 1939) (Br), *Leeina*? sp. (L), *Darvasites* sp. (Da), *Nankinella* sp. (N), *Gyroporella* sp. (Gy) and phylloid algae (Ph), sample TJ170. (E, F) Bioclastic floatstone with monotypic schwagerinoid fusulinids *Shichatenella gundarensis* (Kalmykova, 1960) emend. Bensh, 1987 (S) and rare *Darvasella compacta* (Leven, 1967) (Dv), base of Kubergandian; (E) sample TJ187; (F) sample TJ187.

Fig. 11. Bolorian dasycladaleans and incertae sedis algae. Scale bar = 0.5 mm. (A) Tebagites (concentric crusts of *Archaeolithoporella hidensis* Endo, 1959) with botryoid cements, sample TJ166. (B) *Tubiphytes obscurus* Maslov, 1956 (centre), *Brevaxina dyhrenfurthi* (Dutkevich in Likharev et al., 1939) (bottom left), *Mizzia* sp. (centre top), and microbialite (right), sample TJ171. (C) Aggregate grain with *Mizzia*

sp. (right) and two *Levenella* aff. *leveni* (Kobayashi, 1977) (left, bottom and top), sample TJ171. (D) *Epimastopora japonica* Endo, 1951 (top; longitudinal section) and *Gyroporella microporosa afghanica* Vachard in Vachard and Montenat, 1981 (bottom, oblique section), sample TJ178. (E) *Clavaporella* sp. 2, tangential section in two segments, sample TJ178. (F) *Imperiella* sp., tangential section, sample TJ183.

Fig. 12. Bolorian dasycladaleans and incertae sedis algae. Scale bar = 0.5 mm. (A) *Connexia* sp., transverse section, sample TJ164. (B) *Clavaporella* sp. 1 (Cl1, subaxial section) with *Gyroporella* sp. 1 (Gy) and *Mizzia* cf. *cornuta* Kochansky-Devidé and Herak, 1960 (M), sample TJ163. (C) *Clavaporella* sp. 3 (transitional to *Kochanskyella*?) (Cl3) with two *Globivalvalvulina* sp. (G), sample TJ178. (D) *Clavaporella* sp. 2 (Cl2), *Mizzia* sp. 1 (M), *Brevaxina dyhrenfurthi otai* (Sakaguchi and Sugano, 1966) emend. Ueno, 1991b (Br) and *Endoteba* sp. (En), sample TJ178. (E) *Donezella* cf. *lutugini* Maslov, 1929, large colony preserved in situ, sample TJ169. (F) *Chuvashovia* sp., sample TJ169.

Fig. 13. Bolorian fusulinids and smaller foraminifers. Scale bar = 0.5 mm. (A-D) *Neofusulinella pseudogiraudi* (Sheng, 1962 non 1963), typical axial sections; (A) sample TJ179; (B) sample TJ175; (C) sample TJ175; (D) sample TJ183. (E) *Neofusulinella* sp. 1, axial section, sample TJ179. (F, H) *Toriyamaia* cf. *laxiseptata* Kanmera, 1956; (F) transverse section, sample TJ179; (H) subaxial section, sample TJ164. (G) *Levenella* aff. *leveni* (Kobayashi, 1977) (oblique section, left) (L), *Brevaxina dyhrenfurthi otai* (oblique subtransverse section, right) (Br) and *Mizzia* sp. 1 (M), sample TJ178. (I) *Nodosinelloides* sp., axial section, sample TJ178.

Fig. 14. Bolorian fusulinids and smaller foraminifers. Scale bar = 0.5 mm. (A) *Darvasites contractus* (Schellwien in Schellwien and Dyhrenfurth, 1909), axial section, sample TJ164. (B) *Endoteba* sp., subtransverse section, sample TJ178. (C) *Agathammina*? sp., subaxial section, sample TJ163. (D) *Protonodosaria*? sp., subaxial section, sample TJ182. (E) *Tetrataxis* sp., subaxial section, sample TJ179. (F) *Insolentitheca horrida* (Brazhnikova in Brazhnikova et al., 1967) emend. Vachard in Bensaid et al., 1979, longitudinal section, with a *Neofusulinella* sp. (right) as fundamental and carbonate grains as bricks, sample TJ175. (G) *Neofusulinella* cf. *pseudogiraudi* (Sheng, 1962 non 1963), axial section, sample TJ173. (H)

*Neofusulinella pseudogiraudi* (Sheng, 1962 non 1963), axial section with *Brevaxina* sp. (left), sample TJ175. (I) *Leeina fusiformis* (Schellwien in Schellwien and Dyhrenfurth, 1909), axial section, sample TJ183. (J) *Darvasella* cf. *compacta* (Leven, 1967), oblique axial section, sample TJ187.

Fig. 15. Bolorian *Brevaxina* and *Levenella*. Scale bar = 0.5 mm for (A-K); scale bar = 0.1 mm for (L-N). (A-C, I) *Brevaxina dyhrenfurthi otai* (Sakaguchi and Sugano, 1966) emend. Ueno, 1991b; (A) one transverse and one subaxial section, sample TJ163; (B) oblique subaxial section, sample TJ163; (C) subaxial section, sample TJ163; (I) subaxial section, sample TJ178. (D-F) *Brevaxina dyhrenfurthi* (Dutkevich in Likharev et al., 1939); (D) axial section, sample TJ170; (E) subaxial section, sample TJ171; (F) axial section, sample TJ171. (G, H, J) *Brevaxina parvicostata* (Deprat, 1915); (G) subaxial section, sample TJ173; (H) axial section, sample TJ174; (J) oblique section, sample TJ182. (K) *Brevaxina* sp. 1 transitional to *Misellina termieri* (Deprat, 1915), subaxial section, sample TJ183. (L-M) *Levenella* sp. 1; (L) axial section, sample TJ179; (M) subtransverse section, sample TJ179; (N) *Levenella* aff *leveni* (Kobayashi, 1977), axial section, sample TJ184.

Fig. 16. Biozonation of the Yakhtashian to Murgabian Tethyan stages and proposed correlation with the International (Global) scale.

Fig. 17. *Gundaria insolita* n. gen. n. sp. (A) Section of the conical ventral valve at 0.40 cm from the umbo, specimen MPUM 11524, bed TJ195; (B, C) section of the conical ventral valve respectively at 1.00 and 1.40 cm from the umbo, showing the cystose shell and the section of the muscle lobate mound (in C), specimen MPUM 11525, bed TJ199.

Fig. 18. Reconstruction of *Gundaria insolita* n. gen. n. sp., showing the main internal characters, i.e., the cardinal process in the dorsal valve, the lobate mound for muscle attachment and the cystose shell in the ventral valve and the internal spines.

Fig. 19. *Posicomta gundarensis*. (A) Change in width during the growth of the shell. Two different "trends" characterize the two morphotypes recorded in the fauna from the Gundara Formation. The morphotype A L/W ratio > 1.27 is represented in red,

while the morphotype B L/W ratio < 1.27 is shown in blue. (B) Graph showing how the two morphotypes of *Posicomta gundarensis* are distinctly differentiated based on the L/W ratio.

Fig. 20. Brachiopods of the Gundara Formation. Scale bar = 10 mm for (A) (C) (F) (G) (H) (I) (J) (M) (O) (P) (R) (S) (T) (U) (V) (W) (X) (Y) (Z) (Aa) (Ac) (Ad) (Af) (Ag) (Ah) (Ai) (Ak) (Al) (Am) (An) (Ao); scale bar = 5 mm for (B) (D) (K) (Q) (Ab) (Ae) (Aj); scale bar = 2.5 mm for (E) (L) (N). (A-E) *Gundaria insolita* (MPUM 11410) ventral valve, TJ195; (A) dorsal view; (B) dorsal view with focus on inner details; (C) latero-dorsal view; (D) latero-dorsal view with focus on inner details; (E) myocoelidium. (F) *Gundaria insolita* (MPUM 11411) dorsal view of a ventral valve, TJ195. (G) *Gundaria insolita* (MPUM 11412) lateral view of a ventral valve, TJ195. (H, I) *Gundaria insolita* (MPUM 11413) ventral valve, TJ195; (H) ventral view; (I) lateral view. (J) *Gundaria insolita* (MPUM 11414) lateral view of a section of a ventral valve, TJ195. (K, L) *Gundaria insolita* (MPUM 11415) ventral valve, TJ195; (K) dorsal view; (L) internal view with focus on myocoelidium. (M, N) *Gundaria insolita* (MPUM 11416) ventral valve, TJ195; (M) dorsal view; (N) focus on the spines on the rim of ventral valve. (O, P) *Gundaria insolita* (MPUM 11417) articulated specimen, TJ195; (O) latero-internal view; (P) lateral external view. (Q) *Gundaria insolita* (MPUM 11418) detail of the articulation and cardinal process of an articulated specimen, TJ195. (R, S) *Gundaria insolita* (MPUM 11419) ventral valve, TJ199; (R) lateral view; (S) dorsal view. (T) *Gundaria insolita* (MPUM 11420) dorsal view of an articulated specimen with focus on bases of the rim spines, TJ199. (U-W) *Gundaria insolita* (MPUM 11421) articulated specimen, TJ199; (U) dorsal view; (V) lateral view; (W) antero-dorsal view. (X, Y) *Gundaria insolita* (MPUM 11422) ventral valve, TJ199; (X) dorso-lateral view; (Y) lateral view. (Z, Aa) *Gundaria insolita* (MPUM 11423) articulated specimen, TJ199; (Z) internal lateral view; (Aa) external lateral view. (Ab, Ac) *Gundaria insolita* (MPUM 11424) ventral valve, TJ199; (Ab) dorsal view with focus on internal spines; (Ac) external lateral view. (Ad, Ae) *Gundaria insolita* (MPUM 11425) ventral valve, TJ199; (Ad) external lateral view; (Ae) internal view with focus on internal spines. (Af, Ag) *Gundaria insolita* (MPUM 11426) articulated specimen, TJ199; (Af) lateral view; (Ag) dorsal view. (Ah-Ak) *Gundaria insolita* (MPUM 11427) articulated specimen, TJ199; (Ah) lateral view; (Ai) dorsal view; (Aj) cardinal process; (Ak) oblique-dorsal view. (Al)

*Gundaria insolita* (MPUM 11428) dorso-lateral view of a ventral valve, TJ199. (Am) *Gundaria insolita* (MPUM 11429) dorsal view of a ventral valve, TJ199. (An, Ao) *Gundaria insolita* (MPUM 11430) ventral valve, TJ199; (An) lateral view; (Ao) dorsal view.

Fig. 21. Brachiopods of the Gundara Formation. Scale bar = 10 mm for (A) (B) (D); scale bar = 5 mm for (C) (E). *Gundaria insolita* (MPUM 11431) cluster of several specimens, TJ199. (A) General view; (B) focus on rhizoid spines; (C) detail of one specimen with spines; (D) ventral view of the specimens; (E) Focus on some specimens in ventral view.

Fig. 22. Brachiopods of the Gundara Formation. Scale bar = 10 mm for (A) (C) (N) (Q) (T) (Ac) (Ai) (Aj) (An) (Aq) (Bi) (Bl) (Bp); scale bar = 5 mm for (B) (D) (E) (F) (G) (H) (O) (R) (U) (W) (X) (Y) (Ad) (Ae) (Af) (Al) (Am) (Ao) (Ar) (Aw) (Az) (Bd) (Bf) (Bj) (Bm) (Bq) (Bt); scale bar = 3.33 mm for (Bv); scale bar = 2.5 mm for (I) (L) (M) (P) (S) (Z) (Ab) (Ag) (Ak) (Ap) (At) (Ax) (Ay) (Bb) (Be) (Bg) (Bh) (Bk) (Bo) (Br) (Bs) (Bu); scale bar = 1.25 mm for (J) (K) (V) (Aa) (Ah) (As) (Ba) (Bc) (Bn) (Bw) (Bx). (A-H) *Hemileurus politus* (MPUM 11437) articulated specimen, TJ193; (A) ventral view; (B) ventral view; (C) anterior view; (D) anterior view; (E) lateral view; (F) latero-posterior view; (G) antero-dorsal view; (H) dorsal view. (I, J) *Hemileurus politus* (MPUM 11438) dorsal valve, TJ195; (I) interior details; (J) focus on the divided hinge plate. (K) *Hemileurus politus* (MPUM 11439) hinge plate and crura of a dorsal valve, TJ195. (L) *Hemileurus politus* (MPUM 11440) dorsal view of a ventral valve, TJ195. (M-P) *Hemileurus politus* (MPUM 11441) articulated specimen, TJ195; (M) dorsal view of posterior region; (N) dorsal view; (O) dorsal view; (P) antero-dorsal view. (Q-S) *Hemileurus politus* (MPUM 11442) articulated specimen, TJ195; (Q) ventral view; (R) ventral view; (S) anterior view. (T-Y) *Hemileurus politus* (MPUM 11443) articulated specimen, TJ195; (T) dorsal view; (U) dorsal view; (V) posterior region; (W) anterior view; (X) ventral view; (Y) antero-ventral view. (Z, Aa) *Hemileurus politus* (MPUM 11444) articulated specimen, TJ199; (Z) internal view; (Aa) focus on hinge plate and crura. (Ab) *Hemileurus politus* (MPUM 11445) internal view of an articulated specimen, TJ199. (Ac-Ae) *Posicomta gundarensis* (MPUM 11523) articulated specimen, TJ193; (Ac) lateral view; (Ad) lateral view; (Ae) posterior region. (Af, Ag) *Posicomta gundarensis*

(MPUM 11449) articulated specimen, TJ193; (Af) dorso-lateral view; (Ag) posterior region. (Ah) *Posicomta gundarensis* (MPUM 11450) focus on cardinal plate of a dorsal valve of an articulated specimen, TJ193. (Ai-Ak) *Posicomta gundarensis* (MPUM 11451) articulated specimen morphotype A, TJ194; (Ai) ventral view; (Aj) dorsal view; (Ak) focus on the foramen. (Al-Ap) *Posicomta gundarensis* (MPUM 11452) articulated specimen morphotype B, TJ194; (Al) ventral view; (Am) antero-ventral view; (An) dorsal view; (Ao) dorsal view; (Ap) posterior region. (Aq-At) *Posicomta gundarensis* (MPUM 11453) articulated specimen, TJ194; (Aq) dorsal view; (Ar) dorsal view; (As) focus on the spiralia; (At) dorso-lateral showing the spiralia. (Au, Av) *Posicomta gundarensis* (MPUM 11454) articulated specimen, TJ194; (Au) dorsal view; (Av) dorsal view. (Aw, Ax) *Posicomta gundarensis* (MPUM 11455) articulated specimen, TJ195; (Aw) dorsal view; (Ax) focus on articulation. (Ay) *Posicomta gundarensis* (MPUM 11456) internal view of an articulated specimen, TJ195. (Az, Ba) *Posicomta gundarensis* (MPUM 11457) articulated specimen, TJ195; (Az) ventral view; (Ba) focus on cardinal plate. (Bb, Bc) *Posicomta gundarensis* (MPUM 11458) articulated specimen, TJ195; (Bb) ventral view; (Bc) focus on articulation. (Bd, Be) *Posicomta gundarensis* (MPUM 11459) articulated specimen, TJ195; (Bd) dorsal view; (Be) posterior region. (Bf) *Posicomta gundarensis* (MPUM 11460) ventral valve, TJ197. (Bg, Bh) *Posicomta gundarensis* (MPUM 11461) articulated specimen, TJ197; (Bg) lateral view; (Bh) focus interior details. (Bi-Bk) *Posicomta gundarensis* (MPUM 11462) articulated specimen, TJ197; (Bi) dorsal view, (Bj) dorsal view; (Bk) posterior region. (Bl-Bn) *Posicomta gundarensis* (MPUM 11464) dorsal valve, TJ198; (Bl) ventral view; (Bm) ventral view; (Bn) focus on cardinal plate. (Bo) *Posicomta gundarensis* (MPUM 11463) cardinal plate of a dorsal valve of an articulated specimen, TJ197. (Bp-Bs) *Posicomta gundarensis* (MPUM 11465) articulated specimen, TJ198; (Bp) dorsal view; (Bq) dorsal view; (Br) focus on growth lines; (Bs) posterior region. (Bt, Bu) *Posicomta gundarensis* (MPUM 11466) articulated specimen, TJ198; (Bt) ventral view; (Bu) focus on growth lines. (Bv) *Posicomta gundarensis* (MPUM 11467) ventral view of an articulated specimen, TJ198. (Bw) *Posicomta gundarensis* (MPUM 11468) posterior region of a ventral valve, TJ198. (Bx) *Posicomta gundarensis* (MPUM 11469) dorsal view of an articulated specimen, TJ198.

Fig. 23. Brachiopods of the Gundara Formation. Scale bar = 10 mm for (A) (F) (J) (O) (R) (Y) (Ad) (Al) (Ap) (Ar) (Bc) (Bf) (Bn) (Br); scale bar = 5 mm for (B) (C) (D) (E) (H) (I) (K) (L) (M) (N) (Q) (S) (T) (V) (W) (X) (Aa) (Ab) (Ae) (Ai) (Aj) (Ah) (Am) (An) (Aq) (As) (Au) (Av) (Aw) (Ax) (Ay) (Bd) (Be) (Bg) (Bk) (Bo) (Bp) (Bq) (Bs) (Bu); scale bar = 2.5 mm for (G) (P) (U) (Ac) (Ag) (Ao) (Bb) (Bh) (Bl) (Bt) (Bw); scale bar = 1.25 mm for (Z) (Af) (Ak) (Az) (Ba) (Bi) (Bj) (Bm) (Bv). (A-D) *Orbicoelia* sp. indet. (MPUM 11477) articulated specimen, TJ192; (A) dorsal view; (B) dorsal view; (C) lateral view; (D) latero-posterior view. (E-I) *Orbicoelia* sp. indet. (MPUM 11478) articulated specimen, TJ192; (E) posterior view; (F) ventral view; (G) ventral view; (H) lateral view; (I) anterior view. (J-N) *Orbicoelia* sp. indet. (MPUM 11479) articulated specimen TJ192; (J) dorsal view; (K) dorsal view; (L) anterior view; (M) lateral view; (N) posterior view. (O-Q) *Spiriferellina* sp. indet. (MPUM 11487) ventral valve, TJ193; (O) dorsal view; (P) posterior view; (Q) dorsal view. (R-W) *Spiriferellina* sp. indet. (MPUM 11488) articulated specimen, TJ199; (R) dorsal view; (S) dorsal view; (T) posterior view; (U) focus on the costae; (V) lateral view; (W) ventral view. (X-Z) *Spiriferellina* sp. indet. (MPUM 11489) ventral valve, TJ199; (X) posterior view; (Y) ventral view; (Z) focus on the punctae. (Aa-Ac) *Paraspiriferina* sp. indet. (MPUM 11495) articulated specimen, TJ195; (Aa) lateral view; (Ab) dorsal view; (Ac) dorsal view. (Ad-Ag) *Paraspiriferina* sp. indet. (MPUM 11496) dorsal valve, TJ199; (Ad) dorsal view; (Ae) dorsal view; (Af) focus on costae; (Ag) anterior view. (Ah-Ak) *Paraspiriferina* sp. indet. (MPUM 11497) ventral valve, TJ199; (Ah) posterior view; (Ai) ventral view; (Aj) lateral view; (Ak) focus on imbricated growth lines. (Al-Ao) *Fredericksolasma lata* (MPUM 11499) articulated specimen, TJ195; (Al) dorsal view; (Am) dorsal view; (An) lateral view; (Ao) dorsal view of posterior region. (Ap-As) *Fredericksolasma lata* (MPUM 11503) articulated specimen, TJ198; (Ap) ventral view; (Aq) ventral view; (Ar) latero-ventral view; (As) antero-ventral view. (At-Aw) *Fredericksolasma lata* (MPUM 11500) articulated specimen, TJ197; (At) ventral view; (Au) ventral view; (Av) anterior view; (Aw) lateral view. (Ax-Ba) *Fredericksolasma lata* (MPUM 11501) articulated specimen, TJ198; (Ax) lateral view of a longitudinal section; (Ay) lateral view of the counterpart; (Az) focus on brachidium; (Ba) focus on brachidium. (Bb) *Fredericksolasma lata* (MPUM 11502) posterior region of a ventral valve, TJ198. (Bc-Be) *Fredericksolasma lata* (MPUM 11504) articulated specimen, TJ198; (Bc) dorsal view; (Bd) dorsal view; (Be) anterior view. (Bf-Bh) *Fredericksolasma lata*

(MPUM 11505) articulated specimen, TJ199; (Bf) dorsal view; (Bg) dorsal view; (Bh) posterior region. (Bi, Bj) *Fredericksolasma lata* (MPUM 11506) dorsal valve interior of an articulated specimen, TJ199; (Bi) lateral view of crura, loops and transverse band; (Bj) anterior view of crura, loops and transverse band. (Bk) *Fredericksolasma lata* (MPUM 11507) anterior view of a fragment of an articulated specimen, TJ199. (Bl, Bm) *Fredericksolasma rhomboidalis* (MPUM 11513) fragmented articulated specimen, TJ198; (Bl) anterior view; (Bm) focus on internal features. (Bn-Bq) *Fredericksolasma rhomboidalis* (MPUM 11514) articulated specimen, TJ198; (Bn) ventral view; (Bo) ventral view; (Bp) lateral view; (Bq) antero-ventral view. (Br-Bu) *Fredericksolasma rhomboidalis* (MPUM 11515) articulated specimen, TJ199; (Br) dorsal view; (Bs) dorsal view; (Bt) focus on posterior region; (Bu) antero-ventral view. (Bv) *Fredericksolasma* sp. indet. (MPUM 11521) interior of a fragment of a ventral valve, TJ198. (Bw) *Fredericksolasma* sp. indet. (MPUM 11520) posterior region of a fragment of a ventral valve, TJ198.

Fig. 24. Brachiopods of the Safetdara Formation. Scale bar = 10 mm. (A) *Larispirifer* sp. indet. (MPUM 11482) antero-ventral view of a ventral valve, TJ181. (B) *Larispirifer* sp. indet. (MPUM 11483) ventral view of a ventral valve, TJ181. (C) *Larispirifer* sp. indet. (MPUM 11484) antero-ventral view of a ventral valve, TJ181. (D) *Larispirifer* sp. indet. (MPUM 11485) interior of a ventral valve, TJ181.

Table 1. Lithology and microfacies of the log measured at the Bolorian stratotype section at the junction of the watersheds between the Charymdara, Zydadara and Gundara valleys (38°45’34’’N-70°53’27’’E; 3420 m a.s.l. for the base of the section).

Appendix 1. Biotic content of the samples collected along the Bolorian Stratotype section and the Gundara section.

Appendix 2. Taxonomic notes on dasycladeans, algospongia, smaller foraminifers, primitive fusulinids, Schwagerinoidea and Neoschwagerinoidea by D. Vachard.

Appendix 3. Dimensions in mm of the described brachiopod taxa.

Appendix 4. *Gundaria insolita* n. gen. n. sp. movie by M. Campagna. The 3D reconstruction of the fossil was made using "Sculptris" by Pixologic. The animation of the 3D model was made using "Blender" by Blender Foundation.

| Thickness | Formation name | Lithology | Microfacies |
|---|---|---|---|
| 3 m | Gundara Formation | 20-30 cm-thick bioclastic limestones with interbeds of green marlstones | oncoid/bioclastic FL |
| 5 m | | dark grey marly limestones barren of fossils | |
| 6 m | | yellowish altered fine sandstones | |
| 2.5 m | Safetdara Formation | covered | |
| 3 m | | massive coral limestones | BST, bioclastic WA |
| | | fault | |
| 34 m | | well bedded, 20-40 cm-thick, bioclastic limestones with fusulinids | Oncoid/bioclastic FL, WA, RU |
| 93 m | | poorly outcropping 20-30 cm-thick dark grey bioclastic limestones with oncoids, locally with large spiriferid brachiopods | Oncoid/bioclastic GR |
| 52 m | | covered | |
| 15 m | | poorly outcropping 20-30 cm-thick dark grey bioclastic limestones | Bioclastic GR |
| 15 m | | poorly outcropping shales | |
| 49 m | | poorly outcropping dark grey 25-40 cm thick bioclastic limestones with fusulinids and oncoids (locally with ammonoids) | Bioclastic GR |
| 21 m | | dark grey massive bioclastic limestones with fusulinids, gastropods, bryozoans, crinoids | Bioclastic GR |
| 2 m | | medium bedded bioclastic limestones with fusulinids | Bioclastic FL |

| | | | |
|---|---|---|---|
| 25 m | | white to light grey massive limestones | Microbial BST, bioclastic FL and WA |
| 9 m | | covered | |
| 16 m | | dark grey medium bedded bioclastic limestones with fusulinids, gastropods and large oncoids | Microbial BST, bioclastic GR |
| 130 m | Chelamchi Formation | poorly outcropping shales and sandstones rarely interbedded with bioclastic limestones and yielding olistolithes of massive limestones | Microbial BST, FL |

BST – Boundstone; FL – Floatstone; GR – Grainstone; PA – Packstone; RU – Rudstone; WA – Wackestone.

**Figure 1**

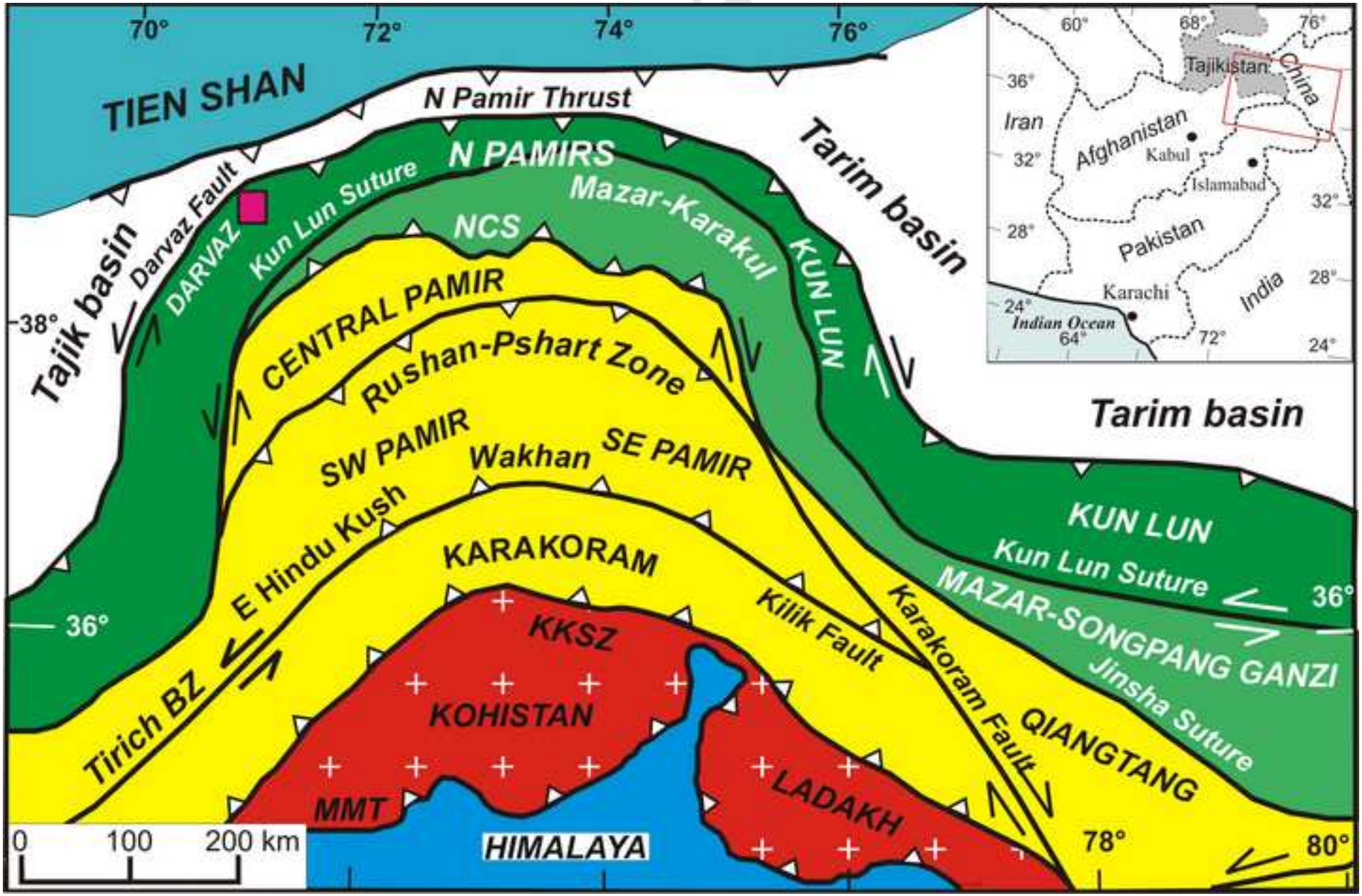
70°
72°
74°
76°
TIEN SHAN
N Pamir Thrust
N PAMIRS
Mazar-Karakul
KUN LUN
Tarim basin
Darvaz Fault
DARVAZ
Kun Lun Suture
Tajik basin
NCS
CENTRAL PAMIR
Rushan-Pshart Zone
SW PAMIR
Wakhan
SE PAMIR
38°
36°
E Hindu Kush
KARAKORAM
Kilik Fault
Karakoram Fault
KUN LUN
Kun Lun Suture
MAZAR-SONGPANG GANZI
Jinsha Suture
QIANGTANG
KKSZ
KOHISTAN
Tirich BZ
MMT
LADAKH
HIMALAYA
78°
80°
0 100 200 km
60°
68°
76°
Tajikistan
China
36°
Iran
Afghanistan
Kabul
32°
Islamabad
28°
Pakistan
Karachi
India
24°
Indian Ocean
64°
72°

Figure 2

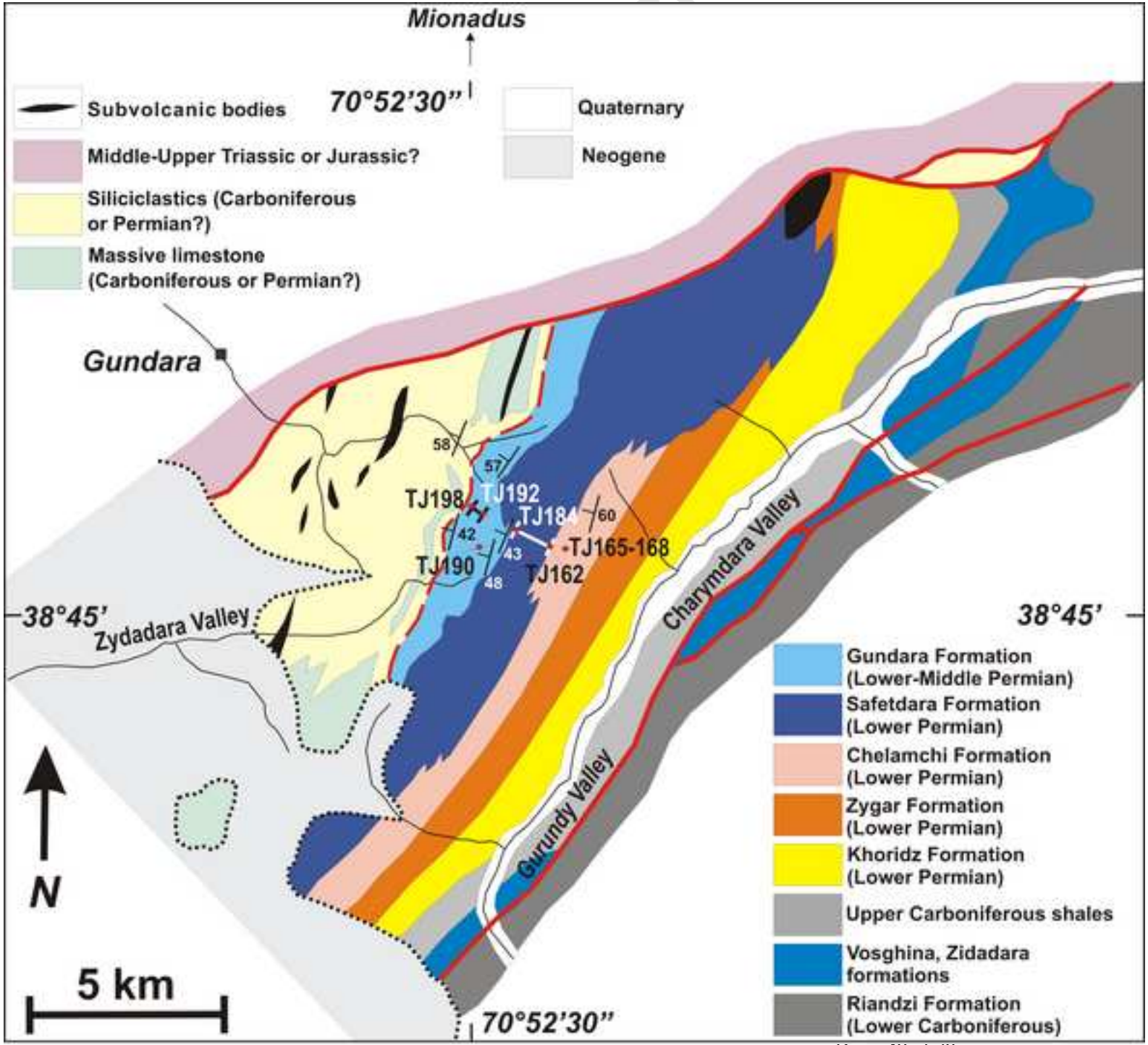
Mionadus
70°52'30"
Subvolcanic bodies
Middle-Upper Triassic or Jurassic?
Siliciclastics (Carboniferous or Permian?)
Massive limestone (Carboniferous or Permian?)
Quaternary
Neogene
Gundara
58
57
TJ198
TJ192
TJ184
60
42
43
-TJ165-168
TJ190
48
TJ162
38°45'
Zydadara Valley
Charymdara Valley
Gurundy Valley
N
5 km
Gundara Formation (Lower-Middle Permian)
Safetdara Formation (Lower Permian)
Chelamchi Formation (Lower Permian)
Zygar Formation (Lower Permian)
Khoridz Formation (Lower Permian)
Upper Carboniferous shales
Vosghina, Zidadara formations
Riandzi Formation (Lower Carboniferous)

**Figure 3**

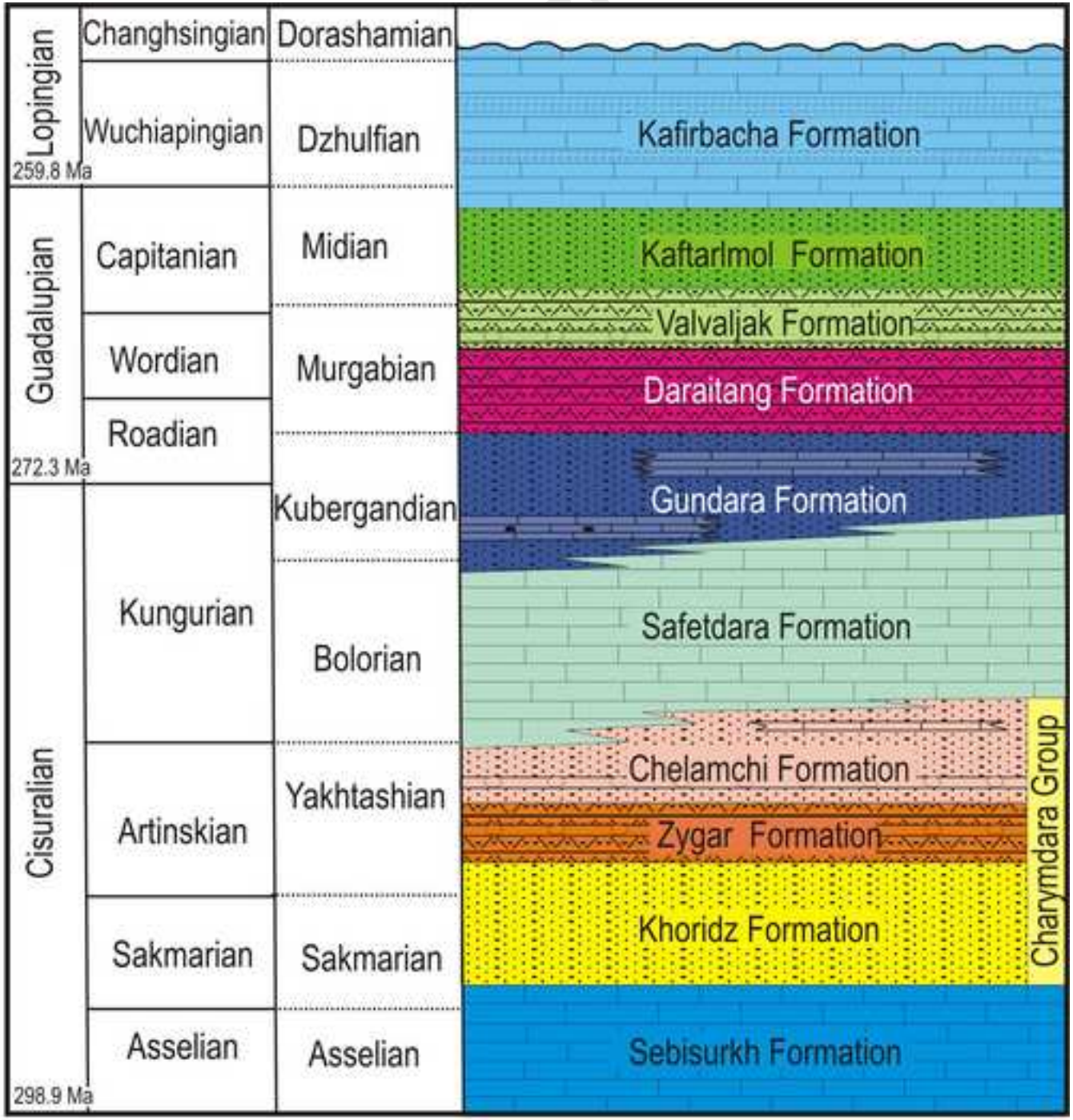
Lopingian
Guadalupian
Cisuralian
259.8 Ma
272.3 Ma
298.9 Ma
Changhsingian
Wuchiapingian
Capitanian
Wordian
Roadian
Kungurian
Artinskian
Sakmarian
Asselian
Dorashamian
Dzhulfian
Midian
Murgabian
Kubergandian
Bolorian
Yakhtashian
Sakmarian
Asselian
Kafirbacha Formation
Kaftarlmol Formation
Valvaljak Formation
Daraitang Formation
Gundara Formation
Safetdara Formation
Chelamchi Formation
Zygar Formation
Khoridz Formation
Sebisurkh Formation
Charymdara Group

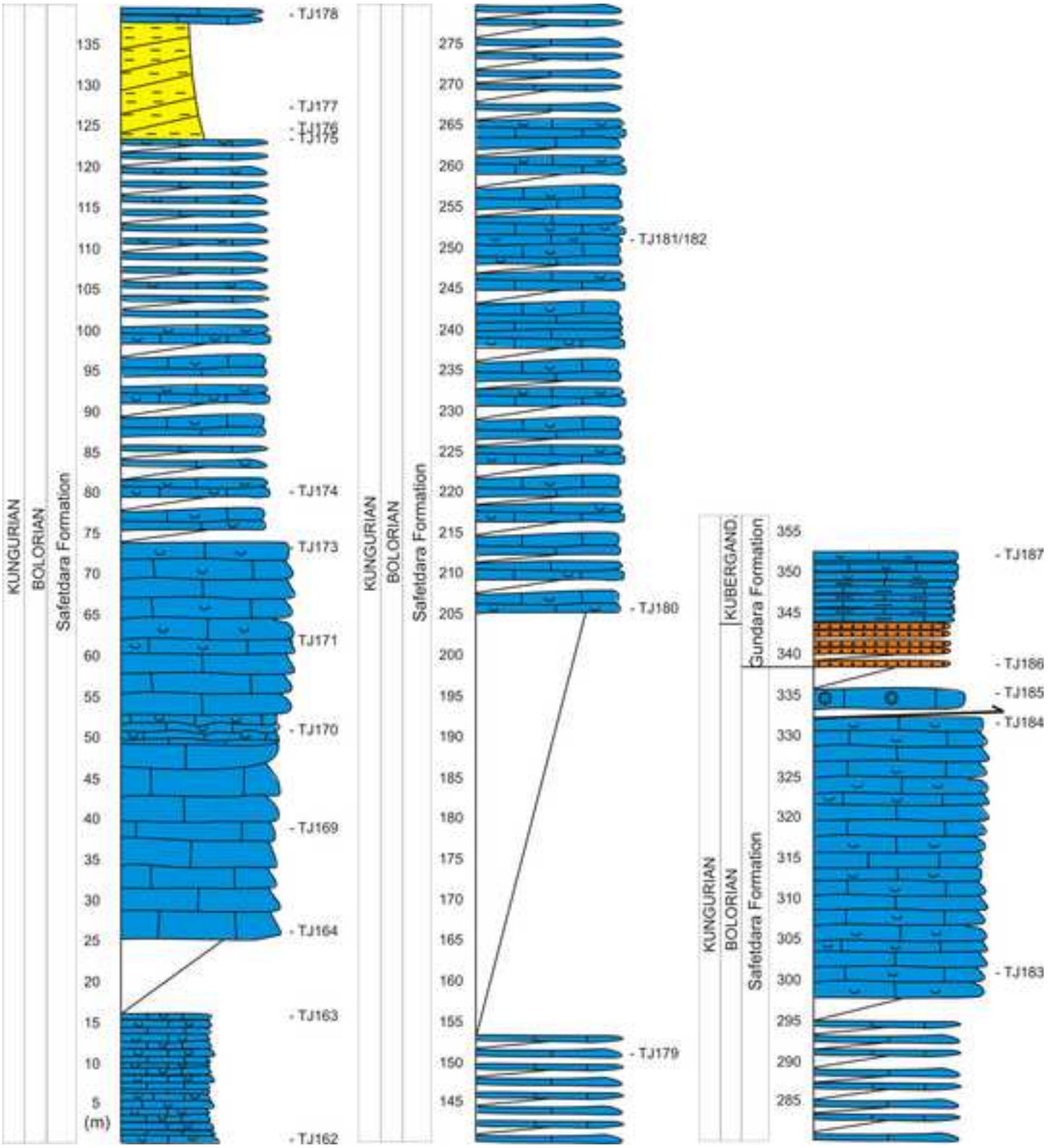

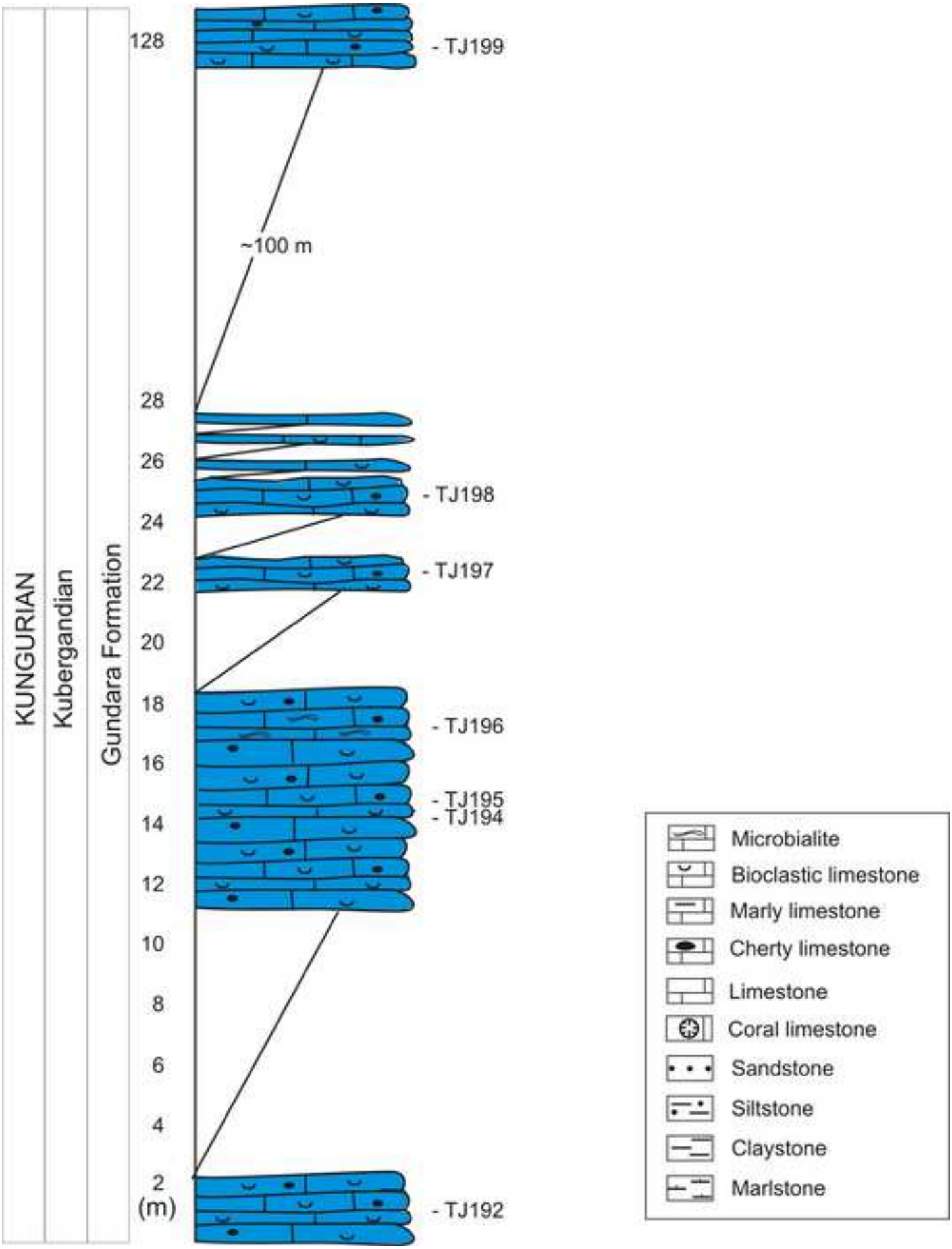

**Figure 6**


S-SW
Safetdara Formation
N-NE
Q.3835
Afghanistan
Panji Valley
Stratotype section
Gurundy Valley
Chelamchi Formation
S
N
Q.3835
Peter the First Range
Obikhingou Valley
Zydadara Valley
massive limestone
Gundara Formation
Gundara section
Gundara Valley
Safetdara Formation

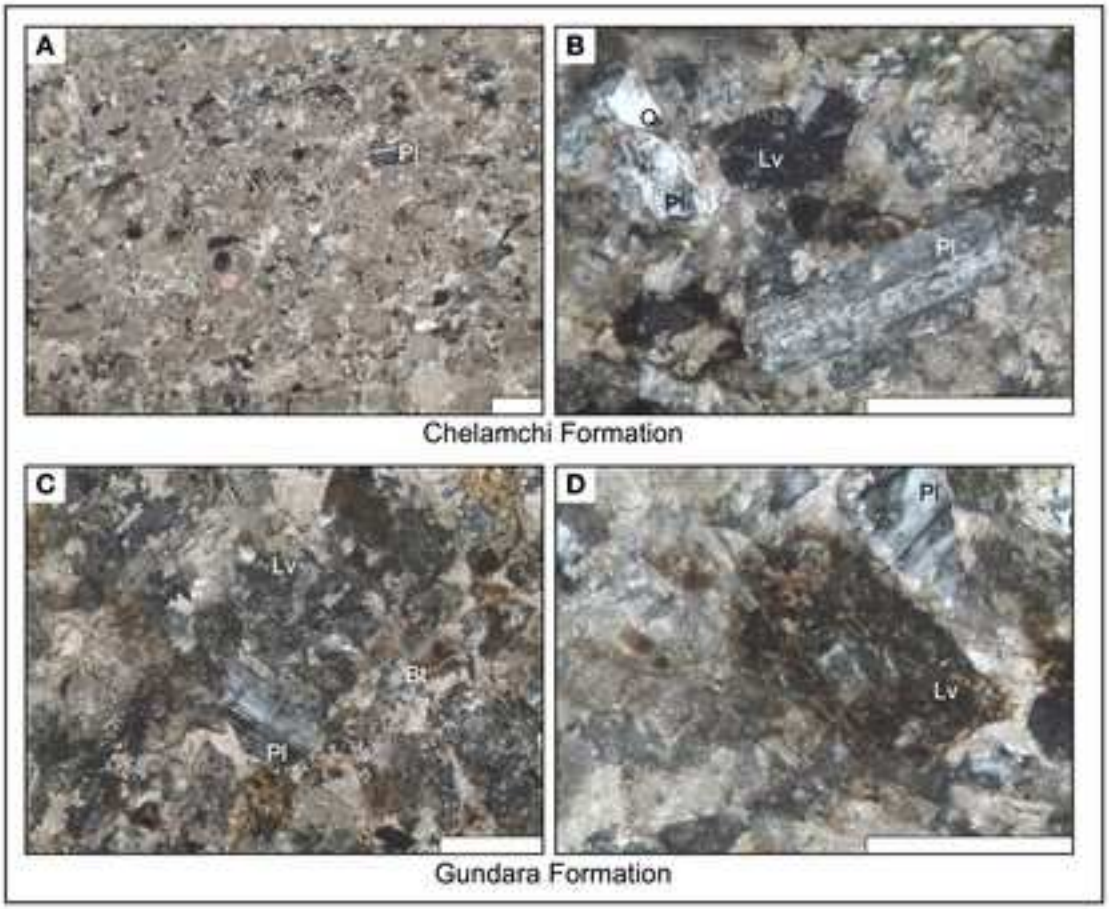

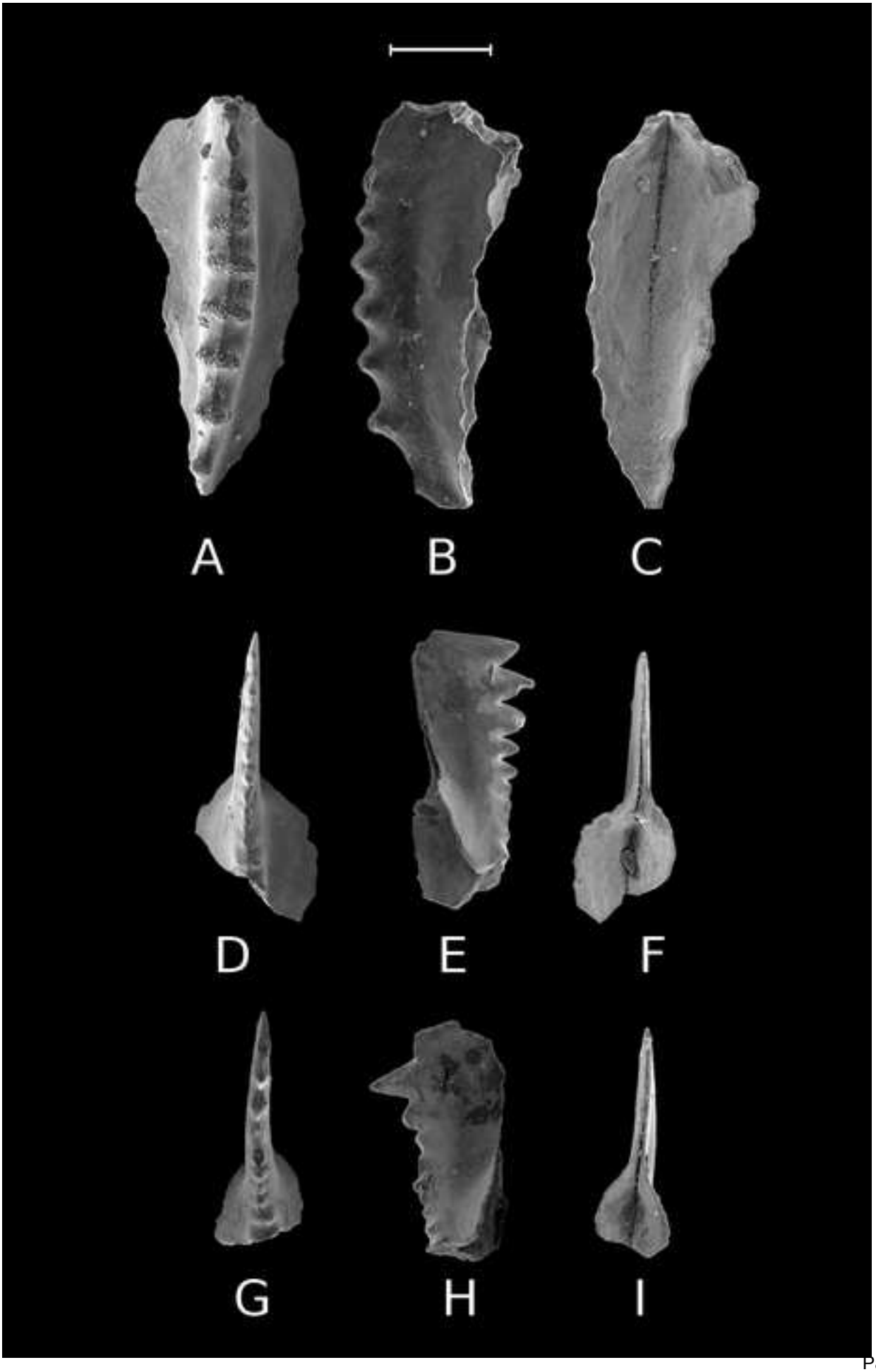

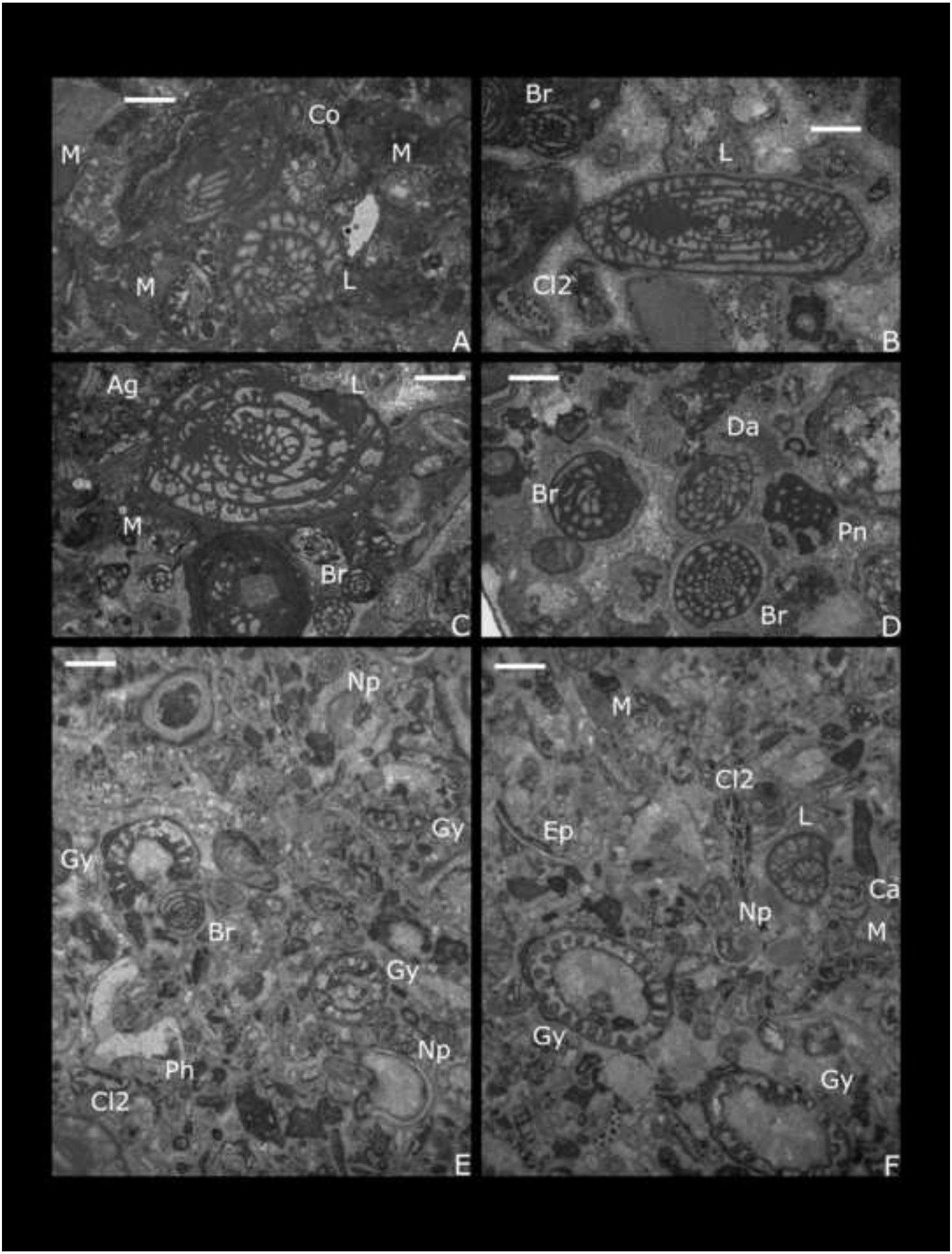

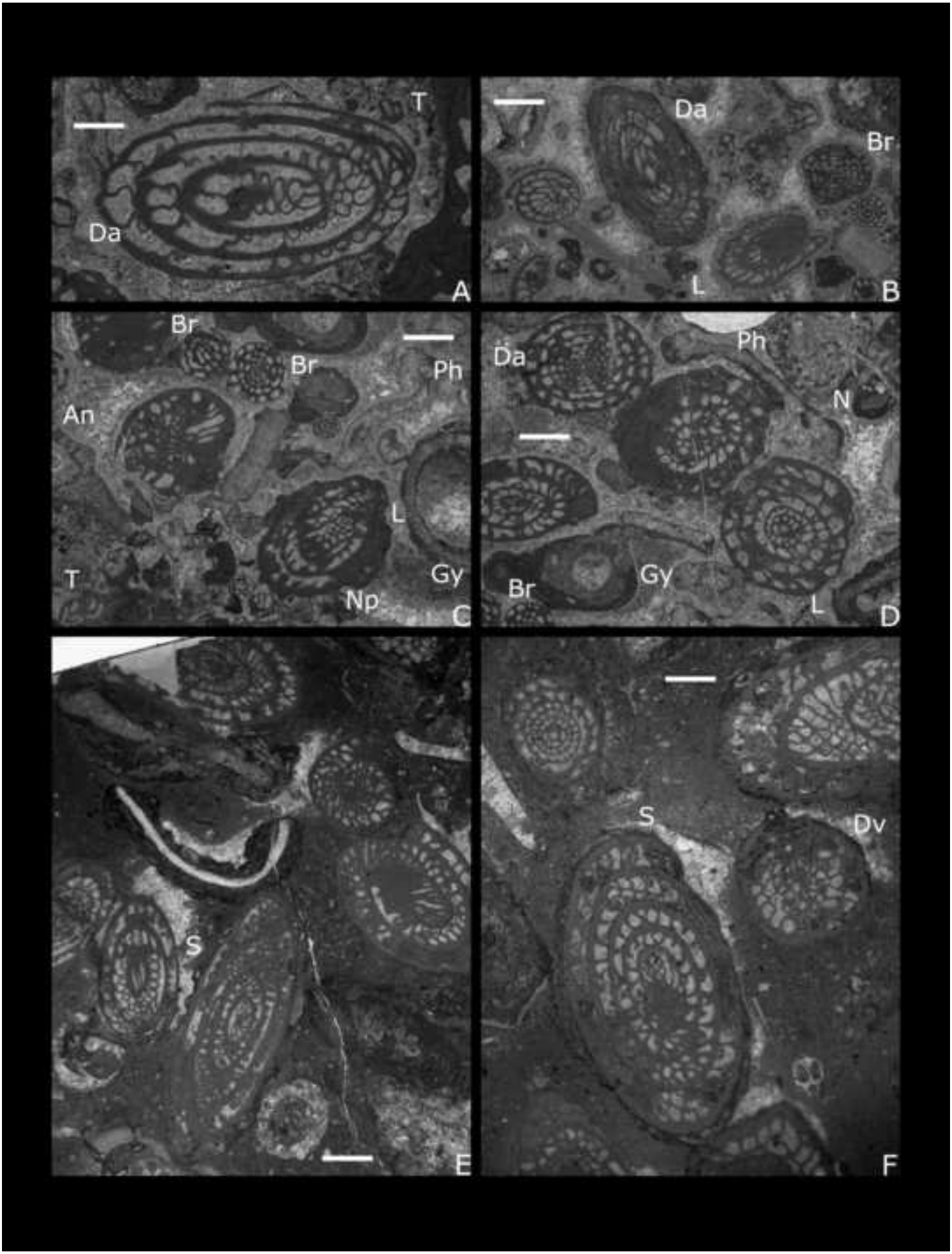

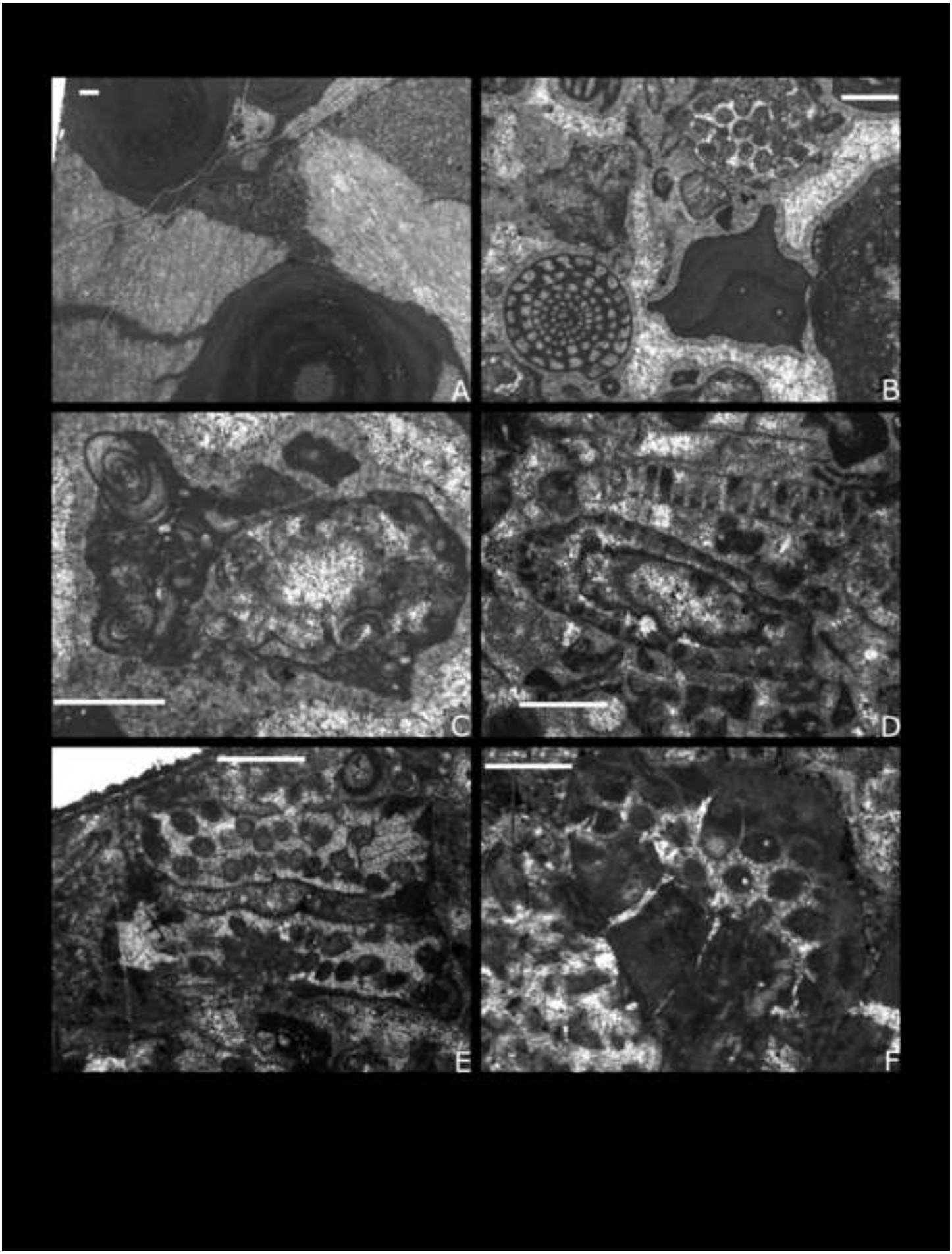

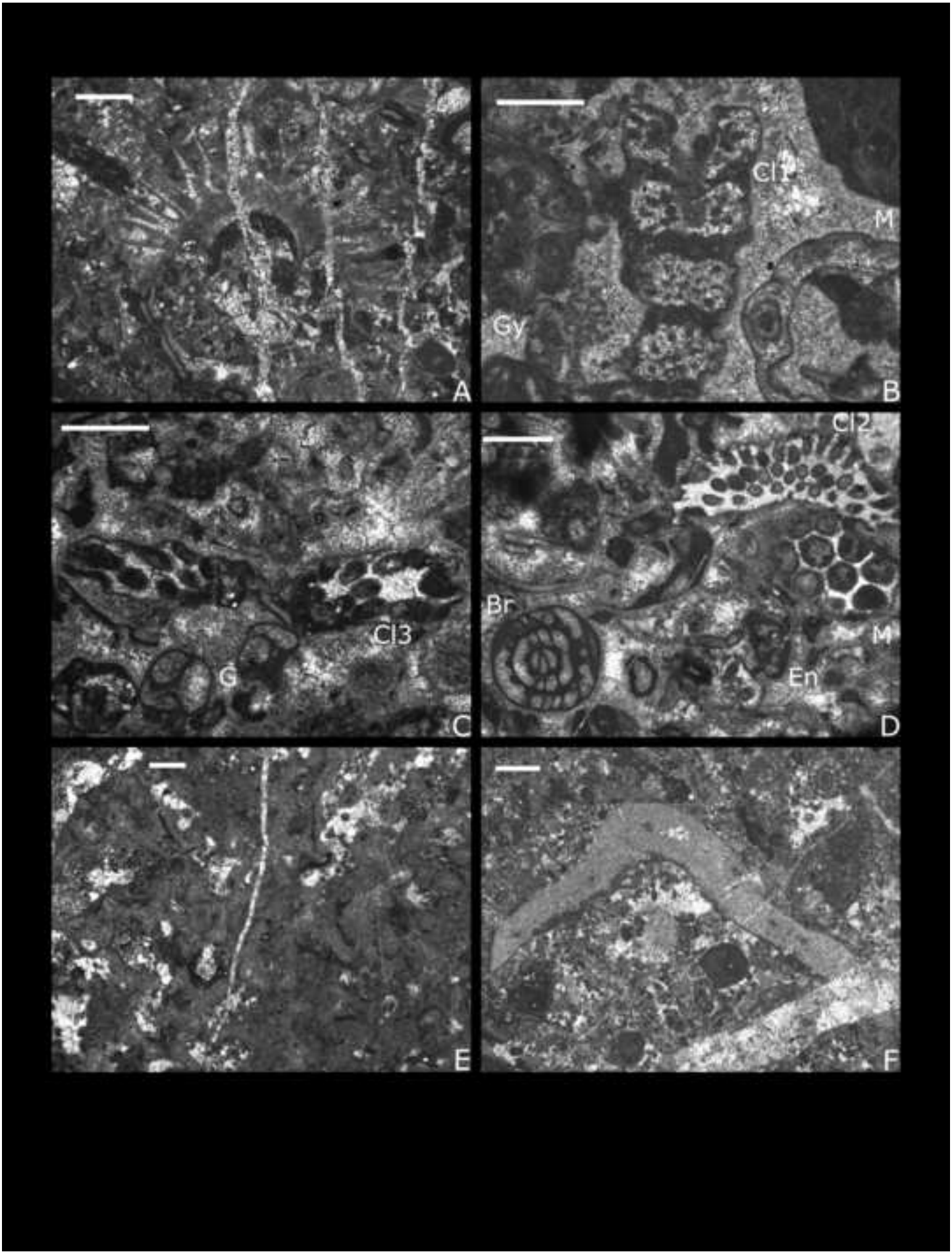

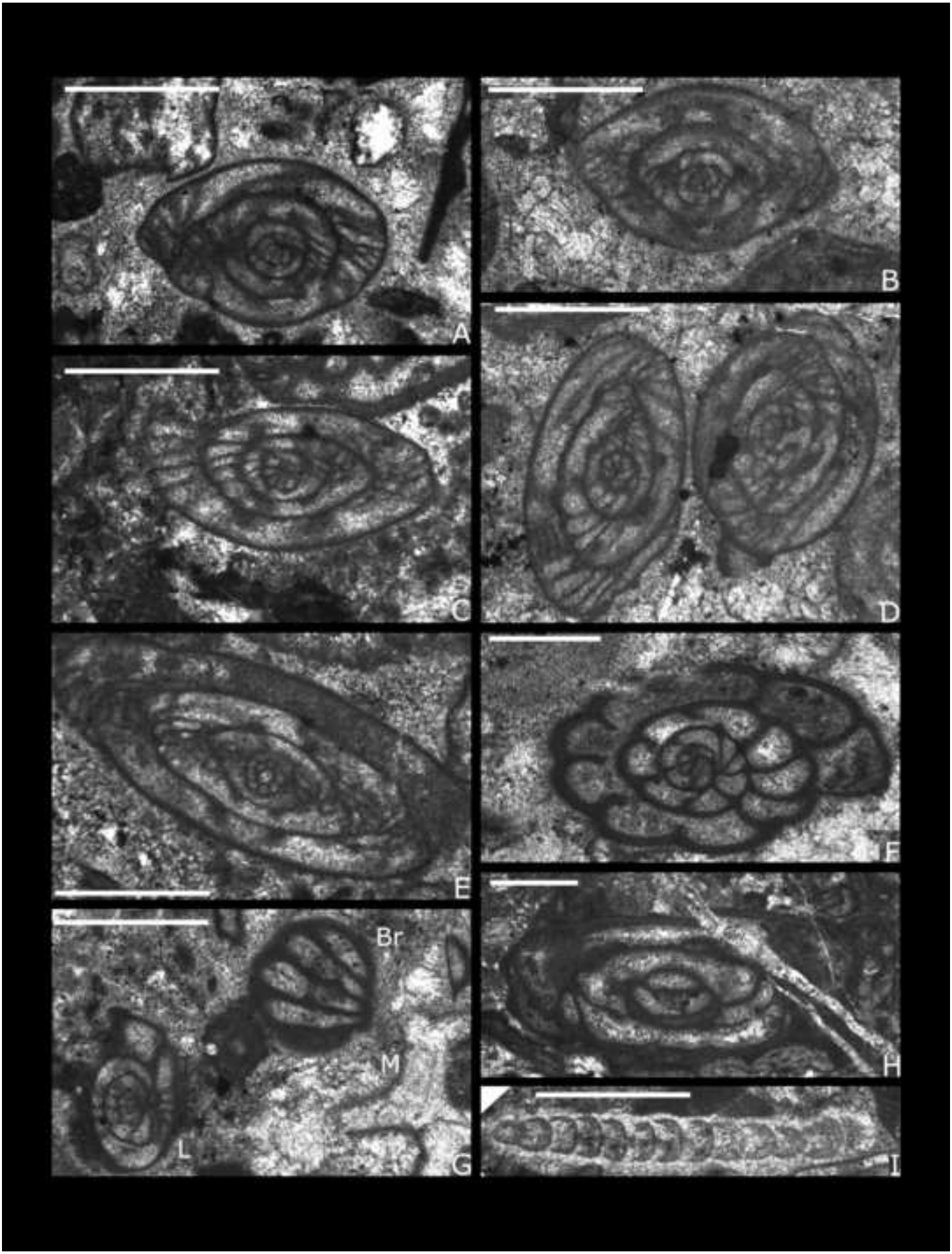

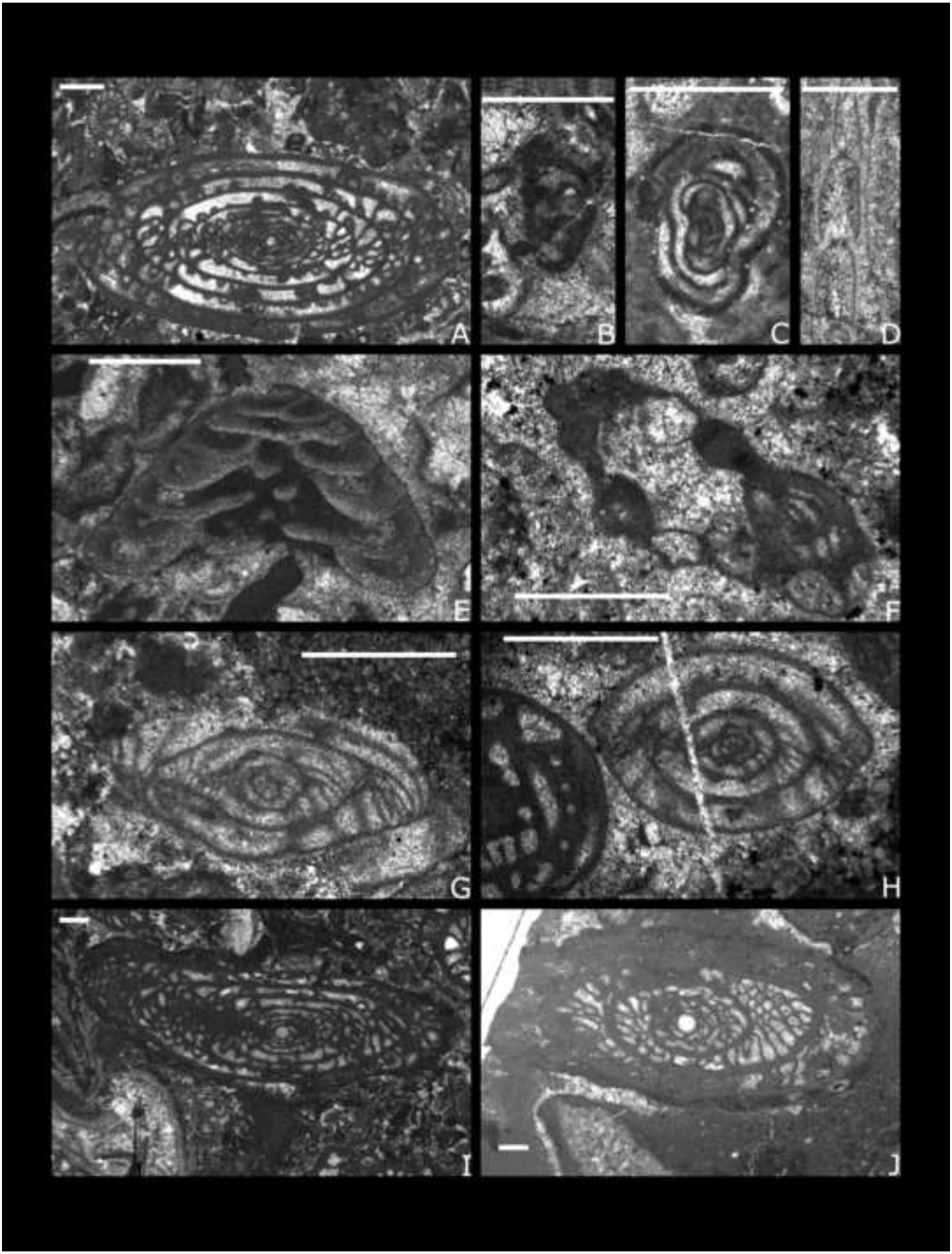

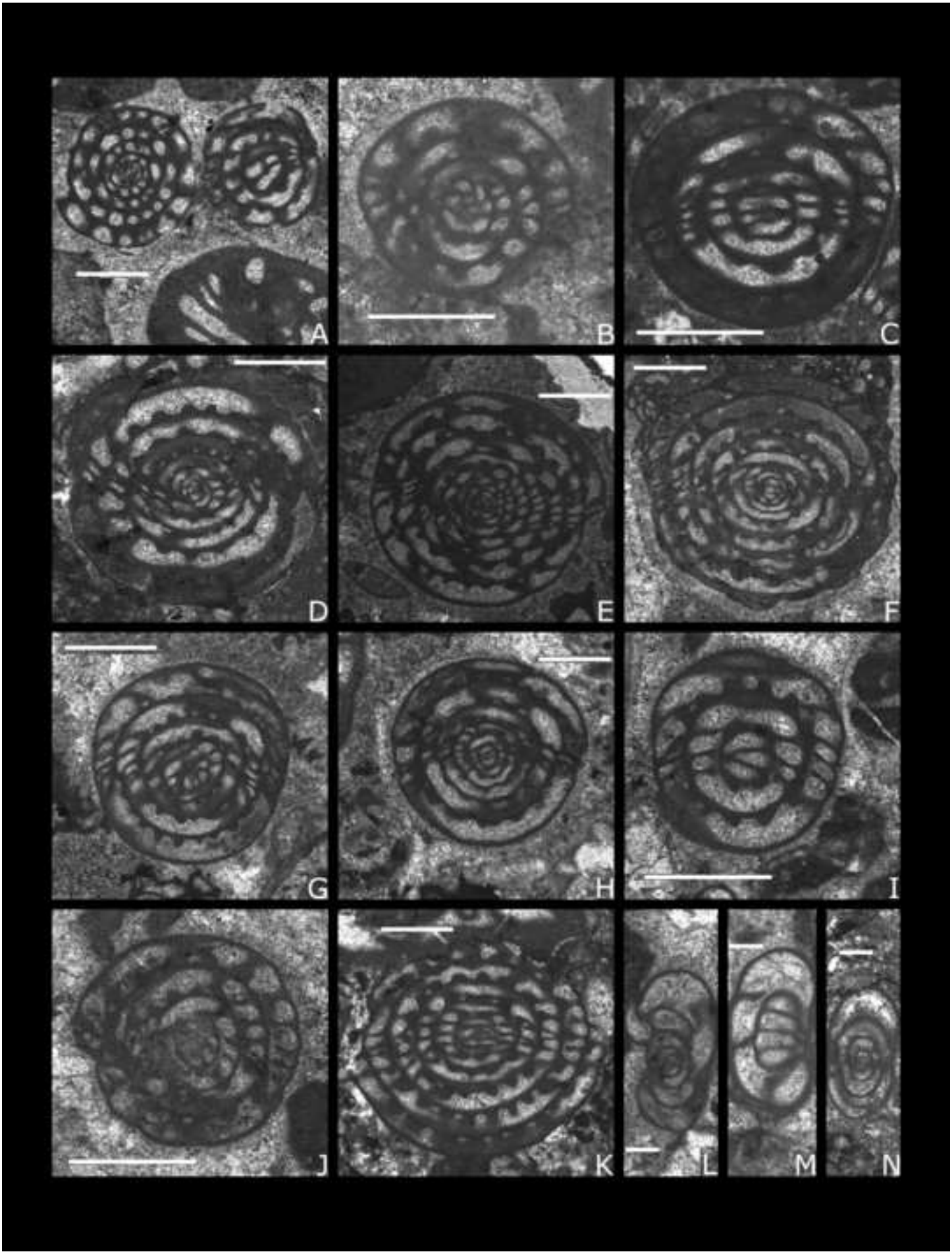

**Figure 16**

| Leven (2001), Leven and Bogoslovskaya (2006) | Ueno (1991b, 1996) | Kobayashi (2005) | Davydov et al. (2013) | This study | Tethyan stages | This study: correlation with the International Time Scale |
|---|---|---|---|---|---|---|
| *N. simplex* | *N. simplex* | *N. simplex* | | *N. simplex* | MURGABIAN | ROADIAN |
| *C. cutalensis*<br>*Armenina, M. ovalis* | *M. claudiae* | *M. pamirica*<br>*M. claudiae*<br>*M. termieri* | *M. claudiae*<br>*A. urtzensis* | *Cancellina*<br>*Misellina* | KUBERGANDIAN | KUNGURIAN |
| *M. termieri*<br>*M. parvicostata*<br>*M. dyhrenfurthi* | *Brevaxina* | *M. dyhrenfurthi* | *M. parvicostata*<br>*M. dyhrenfurthi* | *Brevaxina* | BOLORIAN | |
| zoned by Schwagerinoidea | *Pamirina* | zoned by Schwagerinoidea | *Pamirina* | *Pamirina* | YAKHTASHIAN | ARTINSKIAN |

**Figure 17**

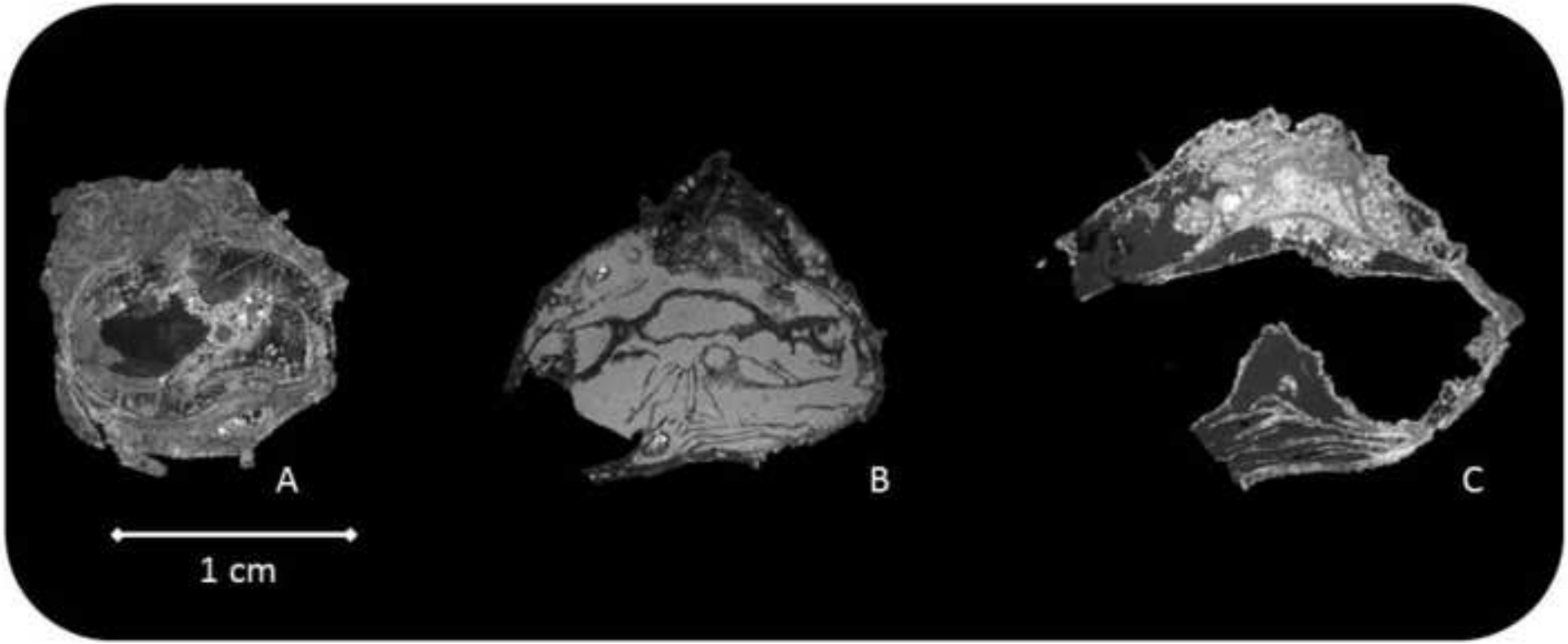

**Figure 18**

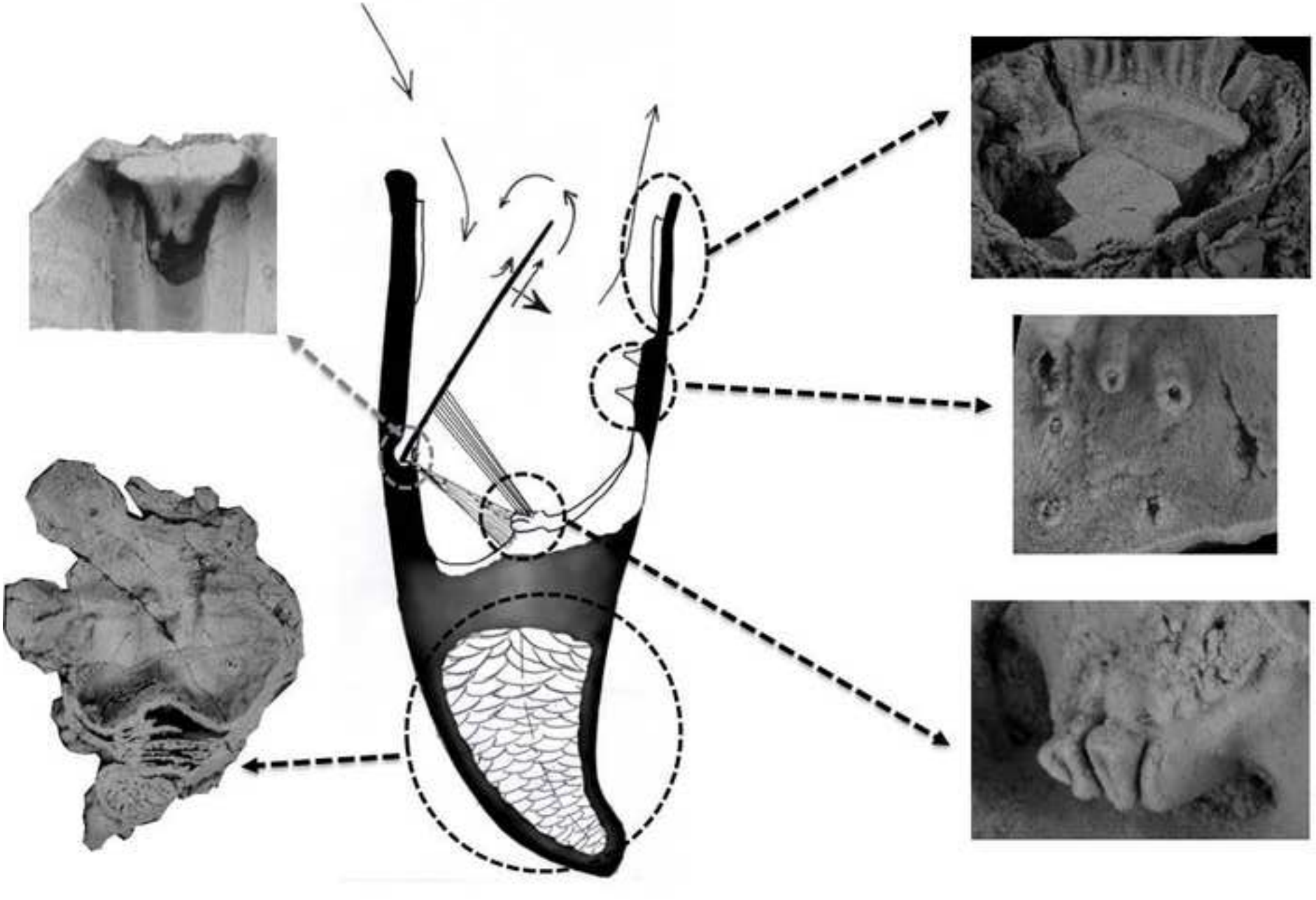

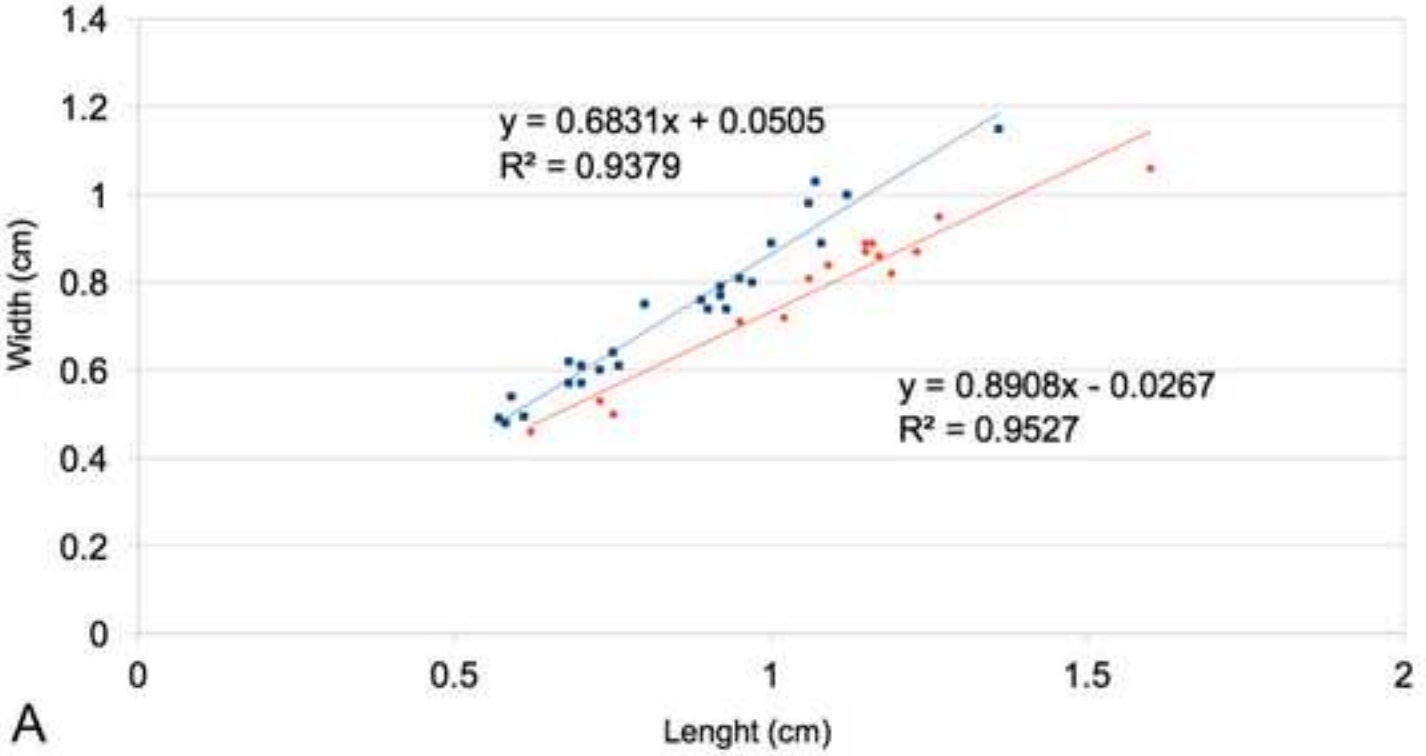


A

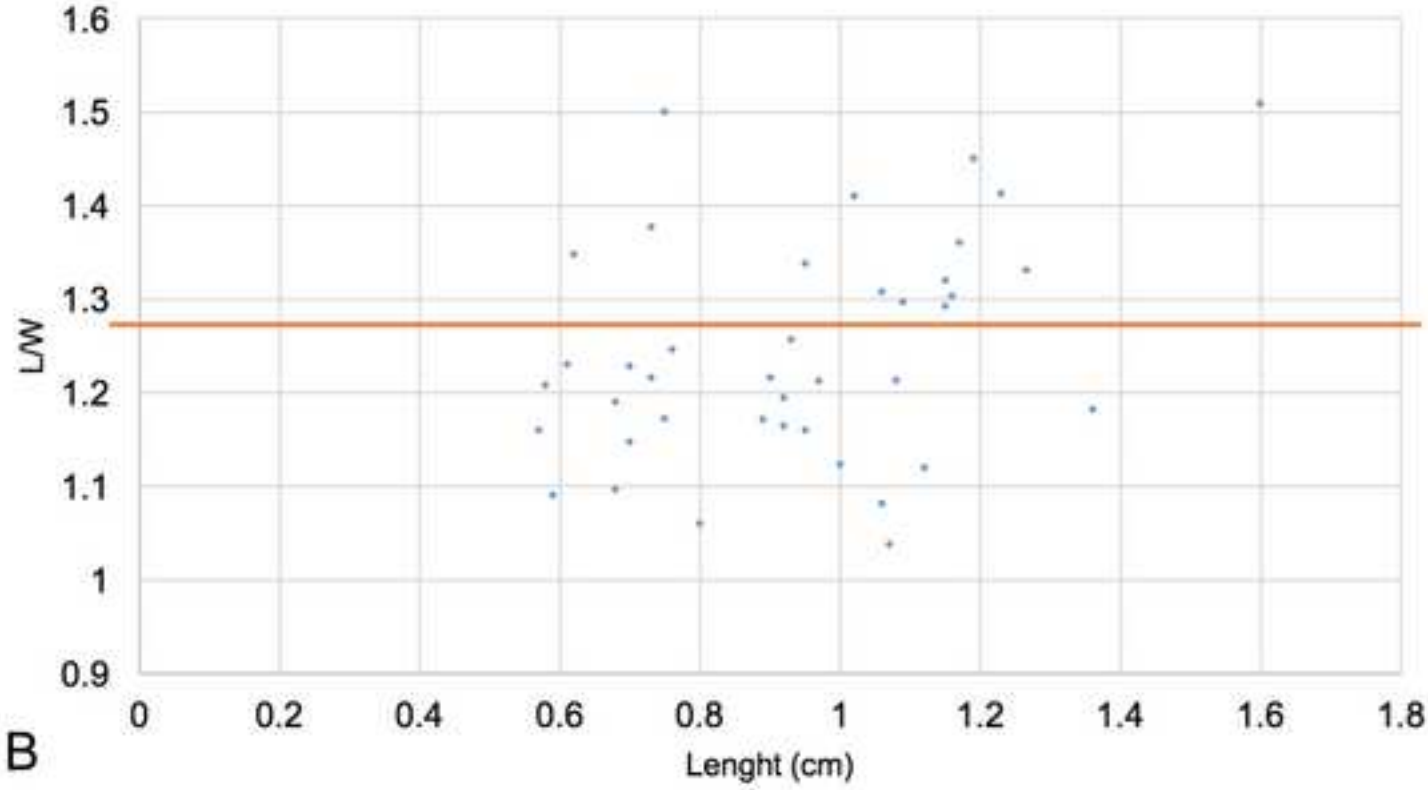


B